

On the fate of a J/ψ produced in a nucleus-nucleus collision

J.-P. Blaizot and J.-Y. Ollitrault

Service de Physique Théorique de Saclay, F-91191 Gif-sur-Yvette, Cedex, France

(Received 13 June 1988)

We examine the possibility that the J/ψ 's produced in nucleus-nucleus collisions could be subsequently destroyed by the inelastic scatterings that they may undergo as they travel across the hot and dense hadronic matter also present in such collisions. The consequences of such an absorption mechanism are then compared with those of a model of J/ψ suppression based on Debye screening of the binding potential in a quark-gluon plasma. One finds that the two mechanisms differ mainly in the way they affect the J/ψ momentum distribution. Impact-parameter effects are analyzed in terms of a simple geometrical model which fits the gross features of nucleus-nucleus collisions. Detailed results are presented for collisions of ^{16}O and ^{32}S projectiles on ^{238}U and ^{65}Cu targets, as well as for ^{208}Pb on ^{208}Pb collisions. These are compared with available experimental data.

I. INTRODUCTION

There is presently considerable interest in the study of J/ψ production in nucleus-nucleus collisions at high energy. This is because the J/ψ is made of heavy quarks which tend to be produced early in the collision and therefore the characteristics of J/ψ production in a nucleus-nucleus collision could reveal some basic properties of the matter in the early stage of the collision. In particular, it has been suggested that, if a deconfined quark-gluon plasma were formed in a collision, one should expect a strong suppression of the J/ψ production.¹ The argument is based on the fact that a quark-gluon plasma at a sufficiently high temperature screens the heavy-quark potential, thus preventing the formation of a bound state. Models based on this idea, and which incorporate essential expected features of the space-time development of a quark-gluon plasma, have been proposed. These models give in particular a definite prediction concerning the way an expanding plasma affects the production of the J/ψ 's, depending on the momentum of the J/ψ 's (Refs. 2-4). The interest in these questions is also strongly motivated by the experimental data obtained recently by the NA38 Collaboration.⁵ These data do indeed suggest that there is some J/ψ suppression in central nucleus-nucleus collisions, with qualitative features which are those expected from the simple models that we have mentioned. However, one should refrain from jumping to conclusions concerning possible evidence for quark-gluon plasma formation, and this for several reasons. First of all, the analysis of the data is not yet in a definite form; in particular the measured suppression is only a relative one with respect to a continuum which is not totally understood. Second, even if one ignores possible ambiguities in the data, one should keep in mind that our theoretical models are still rather crude and many questions remain to be investigated before any firm conclusion could be drawn.

In this paper we shall address questions which are related to the overall space-time development of the system. We shall ignore the very short time processes which could lead to a modification of the $c\bar{c}$ production in a nu-

clear environment [initial-state interactions, European Muon Collaboration (EMC) effect, etc.]. We would like to characterize the reasons why a $c\bar{c}$ pair, created in a nucleus-nucleus collision with the proper kinematical conditions to form a J/ψ , does not lead to a J/ψ . We shall critically examine two apparently distinct models. One is based on the picture of Debye screening: the J/ψ is suppressed because the potential which binds a $c\bar{c}$ pair is screened by the quark-gluon plasma. In the other model, one tries to account for J/ψ suppression by invoking inelastic scattering of the J/ψ , or more properly of the $c\bar{c}$ system, on other particles which are copiously produced in a nucleus-nucleus collision; one assumes then that each collision breaks the $c\bar{c}$ pair, thus preventing the formation of the bound state. In both cases, we shall investigate the interplay between the space-time development of the matter and the microscopic mechanism of J/ψ suppression. For simplicity, we shall restrict our consideration to the central rapidity region.

In order to compare the model predictions to experimental data, we shall rely on the fact that the bulk features of nucleus-nucleus collisions at high energy are dominated by elementary geometrical effects. Thus, quantities such as the transverse energy produced in the collision, or the multiplicity in the central rapidity region, can be related in a straightforward way to the impact parameter. This will allow us to discuss noncentral collisions in a simple fashion. The comparison with the available data will lead us to critical conclusions. On the one hand, the model based on Debye screening is found to be able to account for most of the data; however, the resulting values of the parameters are such that the microscopic picture is not at all convincing. On the other hand, the model based on J/ψ absorption could be pushed to describe part of the data, but not all; and there too one runs into a problem of interpretation: the densities of the scatterers which are involved are so large that it does not make sense any more to think of them as real hadrons.

Let us mention that the possibility of J/ψ absorption by a nuclear medium has been considered recently by several other groups.⁶⁻¹⁰ In Refs. 6 and 7 one attempts

to relate the J/ψ suppression observed in nucleus-nucleus to the absorption found in proton-nucleus collisions. The other works⁸⁻¹⁰ are close to what we do and actually contain some of our intermediate results. However, our analysis is more complete. We give in particular a full treatment of the transverse expansion and we study the dependence of the results on target and projectile masses and on the observables of the collision: namely, the total transverse energy and the J/ψ transverse momentum. Also, we would like to point out our disagreement about one conclusion reached in Refs. 8 and 9. It is found there that the effect of absorption cuts off when the J/ψ momentum exceeds a certain value. This is in contrast with our finding that the absorption actually depends very little on p_T . The origin of this discrepancy lies in the fact that those authors are introducing a J/ψ formation time and assume that absorption sets in only after that time. This point will be discussed in Sec. II. Let us finally indicate that the propagation of a $c\bar{c}$ system in a quark-gluon plasma has been considered in Ref. 11 from a different point of view. Also, the change in $c\bar{c}$ production due to the nuclear environment has been calculated in Ref. 12.

Let us now indicate the plan of this paper. In Sec. II we isolate and study several physical effects which have to be taken into account when describing the interaction of a $c\bar{c}$ pair with an expanding hadronic fluid. In Sec. III we recall the main features of the model for J/ψ suppression by a quark-gluon plasma which has been developed in Ref. 3. In both Secs. II and III the fraction of surviving J/ψ 's is calculated as a function of dimensionless parameters; this allows us to extract a universal behavior for each model. In Sec. IV we relate our calculations to experimental quantities: using a simple model for particle production in the collision, we compute the fraction of J/ψ suppression as a function of the transverse energy. The free parameters of our models are fitted to experimental results for oxygen-uranium, and predictions are done for other types of collisions. Our conclusions are summarized in Sec. V.

II. ABSORPTION OF A J/ψ BY AN EXPANDING HADRON FLUID

For simplicity, we shall consider in this section, as well as in Sec. III, only ideal central collisions of identical nuclei at very large energy. Collisions involving nonidentical nuclei at nonzero impact parameter will be treated in Sec. IV.

We assume that $c\bar{c}$ pairs are created in hard processes, which last a very short time, of the order of $1/2m_c \lesssim 0.1$ fm/c, m_c being the mass of a charm quark ($m_c \gtrsim 1$ GeV). These processes take place at the very beginning of the collision. There is, of course, some ambiguity in what we call the beginning of the collision, since in the center-of-mass frame, it takes a time of the order of $2R_0/\gamma$ for the two nuclei to cross each other, R_0 being the radius of one nucleus and γ the Lorentz contraction factor. For definiteness, we shall call $t=0$ the time at which the two nuclei have maximum overlap and consider that the $c\bar{c}$ pairs appear at that time, assuming that the γ factor is large enough so that the aforementioned ambiguity can be ignored. In the same spirit, we shall also assume that

all the pairs are created, and remain, in a plane at $z=0$ perpendicular to the collision axis, that is we consider only those pairs which have no longitudinal momentum. We call p_T the transverse momentum of a pair.

Once a $c\bar{c}$ pair has been created, it takes some time, which we call t_ψ , before a J/ψ appears as a bound state in the system. It is sometimes argued that because the $c\bar{c}$ is such a small system when it is first created, it does not interact much with the surrounding medium; then all interactions are ignored before time t_ψ . On the other hand, in models of absorption of a J/ψ by nucleons, it is implicitly assumed that the absorption takes place as soon as the $c\bar{c}$ is created;^{6,7} if it were not so, no absorption would take place since one finds that the J/ψ is formed outside the nucleus, whatever reasonable value is chosen for the formation time t_ψ . The estimates of the ψ -nucleon absorption cross section,¹³ used, for example, in Refs. 6 and 7, refer thus to an interaction between the nucleon and the $c\bar{c}$ system at a time where this system is not yet really a J/ψ . This point has also been emphasized in Ref. 14. We shall therefore take the view that absorption can set in as soon as the $c\bar{c}$ quark-antiquark pair is created. We shall ignore in this paper the absorption which results from interaction of the $c\bar{c}$ system with the nucleons in both nuclei. This has been estimated in Refs. 6 and 7 and found to account for a sizable ψ suppression. In a complete, quantitative estimate, that should therefore be taken into account. We shall concentrate here only on the absorption which could take place in the central rapidity region as soon as hadronic matter, or a quark-gluon plasma, has been formed there.

Continuing our discussion of time scales, we now consider the time t_0 at which matter starts to appear in the central rapidity region. It cannot be smaller than typically half the crossing time of the two nuclei, if we take for time $t=0$ the time at which the two nuclei have maximum overlap. This minimum value is the one which we shall adopt in our work and, in particular, in Sec. IV. Whatever absorption takes place before t_0 may be considered as absorption by the nucleons of the nuclei and this is ignored here. One should note that, if one insists on having real hadrons in the central region, t_0 should be taken to be somewhat longer than the value we are choosing, in order to account for the hadron formation time which may be typically 1-2 fm/c (Ref. 15). Finally, we shall assume that at time t_0 the matter is thermalized. This allows us to perform detailed calculations of the evolution of the system.

As soon as it is produced, the $c\bar{c}$ system starts to interact with the nucleons of both target and projectile nuclei, and also with the other particles produced in the collision; we assume that the latter form either a quark-gluon plasma or a hot gas of hadronic resonances. For the sake of simplicity we shall consider mainly pions in this paper, although heavier mesons may constitute a large fraction of hadronic matter at high temperatures. In fact, we shall indeed, for definiteness, refer to pions as the objects on which the $c\bar{c}$ system scatters inelastically; however, we shall see that most of our results, and also our main conclusions, are actually independent of the precise nature of the scatterers. We shall describe the in-

teraction between J/ψ 's and pions as an incoherent sum of individual collisions. Since the elastic cross section is expected to be small in comparison with the inelastic one,¹³ we shall ignore elastic collisions and assume that each collision of the $c\bar{c}$ system inhibits the formation of the J/ψ . We shall call $f(\mathbf{r}, \mathbf{p}_T, t)$ the distribution of J/ψ 's in phase space (in the same way as we shall often call pions the scatterers, we shall not always, unless needed, distinguish the " J/ψ " from the " $c\bar{c}$ system" from which it originates); because of our assumptions, the position \mathbf{r} and the momentum \mathbf{p}_T of the J/ψ are vectors in the $z=0$ plane. We write for f the following simple kinetic equation:

$$\frac{\partial f}{\partial t} + \mathbf{v} \cdot \nabla f = -f \int \frac{d^3 p'}{(2\pi)^3} f_\pi(\mathbf{r}, \mathbf{p}', t) \sigma v_{\text{rel}} \frac{\mathbf{p} \cdot \mathbf{p}'}{EE'}, \quad (2.1)$$

$$f(\mathbf{r}, \mathbf{p}_T, t) = f_0(\mathbf{r} - \mathbf{v}t, \mathbf{p}_T) \exp \left[- \int_0^t dt' \int \frac{d^3 p'}{(2\pi)^3} f_\pi(\mathbf{r} - \mathbf{v}(t-t'), \mathbf{p}', t') \sigma v_{\text{rel}} \frac{\mathbf{p} \cdot \mathbf{p}'}{EE'} \right]. \quad (2.3)$$

The total J/ψ suppression factor due to inelastic scattering with pions is given by

$$\mathcal{A}(\mathbf{p}_T) = 1 - \frac{\int d^2 r f(\mathbf{r}, \mathbf{p}_T, t = +\infty)}{\int d^2 r f_0(\mathbf{r}, \mathbf{p}_T)} \equiv 1 - \mathcal{N}(\mathbf{p}_T) \quad (2.4)$$

and \mathcal{N} is the probability that the J/ψ escapes the system. We shall, furthermore, assume that the distribution $f_0(\mathbf{r}, \mathbf{p}_T)$ factorizes into $f_0(\mathbf{r})g(\mathbf{p}_T)$.

Finally, in order to compute the suppression factor, an expression for the pion distribution function is required. As already mentioned, we assume that the pion fluid quickly reaches local equilibrium, and that its expansion is governed by the laws of hydrodynamics for ideal fluids. If $u^\mu(\mathbf{r}, t)$ is the fluid four-velocity and $T(\mathbf{r}, t)$ the temperature at point \mathbf{r} and time t , $f_\pi(\mathbf{r}, \mathbf{p}', t)$ is simply the Bose-Einstein distribution for noninteracting particles:

$$f_\pi(\mathbf{r}, \mathbf{p}', t) = \frac{3}{\exp(p'_\mu u^\mu / T) - 1}, \quad (2.5)$$

where the factor 3 is the degeneracy factor for pions. The mass of the pion is a small quantity which can most often be ignored. In this case the relative velocity is always 1 and Eq. (2.1) takes a simple form:

$$\frac{\partial f}{\partial t} + \mathbf{v} \cdot \nabla f = -f \sigma n (1 - \mathbf{v}_f \cdot \mathbf{v}), \quad (2.6)$$

where n is the fluid density,

$$n(\mathbf{r}, t) = \int \frac{d^3 p'}{(2\pi)^3} f_\pi(\mathbf{r}, \mathbf{p}', t), \quad (2.7)$$

and \mathbf{v}_f the fluid velocity:

$$\mathbf{v}_f(\mathbf{r}, t) = \frac{1}{n(\mathbf{r}, t)} \int \frac{d^3 p'}{(2\pi)^3} f_\pi(\mathbf{r}, \mathbf{p}', t) \frac{\mathbf{p}'}{E'}. \quad (2.8)$$

In this paper, we shall use the hydrodynamical model developed in Refs. 16 and 17 which allows a complete

description of the longitudinal and transverse expansion of the fluid produced in the central rapidity region.

Since several physical effects mix in the solution of Eq. (2.1), we shall, for pedagogical purposes, explore a few special cases, in order of increasing complexity. We shall first study absorption by a static, uniform pion gas (Sec. II A). At this point, several effects can be discussed: when the temperature is raised, both the total number of pions and their average velocity increase, which results in an increase of the absorption; another effect is the dependence of absorption on the threshold of the reaction: such a threshold cuts off the absorption of low- p_T J/ψ 's. In Sec. II B we consider a uniform pion gas undergoing regular cooling, according to Bjorken's law for the longitudinal expansion.¹⁶ We show that, because of the slow decrease of the pion density ($n \propto 1/t$), the absorption is total for large times. In fact, at a time of order R_0 , two effects contribute to cut off the absorption. First, the transverse expansion strongly accelerates the cooling, i.e., the dilution of the pion fluid. Second, $c\bar{c}$ pairs which have large velocities, i.e., large p_T , start to leave the interaction region; this finite-size effect decreases the absorption at large p_T , in contrast with the effects of threshold and relative velocity discussed above. In Sec. II C we give a full treatment of these two effects (transverse expansion, finite size) and we derive an approximate simple formula for $\mathcal{N}(p_T)$.

A. J/ψ in a static pion gas

We start by considering the absorption of a J/ψ by a static, uniform pion gas in thermal equilibrium at a temperature T . The distribution function for noninteracting pions, given by Eq. (2.5), reduces to

$$f_\pi(E) = \frac{3}{\exp(E/T) - 1}, \quad (2.9)$$

where E is the pion energy. The distribution function of

\bar{c} then takes the simple form

$$f(\mathbf{r}, \mathbf{p}_T, t) = f_0(\mathbf{r} - \mathbf{v}t, \mathbf{p}_T) \exp(-t/\theta), \quad (2.10)$$

where θ , the collision time, is given by

$$\frac{1}{\theta} = \int \frac{d^3p'}{(2\pi)^3} f_\pi(E') \sigma v_{\text{rel}} \frac{\mathbf{p} \cdot \mathbf{p}'}{EE'}. \quad (2.11)$$

The integral in (2.11) can be easily evaluated if E' and $\mathbf{p} \cdot \mathbf{p}'$ are taken as integration variables. A quick calculation then gives

$$\frac{1}{\theta} = \int dE' f_\pi(E') \int \frac{d(\mathbf{p} \cdot \mathbf{p}')}{(2\pi)^2} \sigma v_{\text{rel}} \frac{\mathbf{p} \cdot \mathbf{p}'}{EE'}. \quad (2.12)$$

In order to estimate (2.12) numerically, we assume that σ has a constant value above threshold, that is when $(p+p')^2 > M_0^2$, where M_0 is the mass of the reaction products. Then the integral over $\mathbf{p} \cdot \mathbf{p}'$ can be carried out very easily.

Figure 1 displays the absorption rate $1/\theta$, for different values of the temperature, and as a function of the J/ψ momentum p_T , in the case where there is no reaction threshold, that is $M_0 = m_\pi + M$ (solid line), and for a threshold at 498 MeV corresponding to the reaction $\psi\pi \rightarrow D\bar{D}$ (dashed line). The temperature dependence of the rate is seen to be quite appreciable; this is due to the fact that the pion density is a rapidly growing function of T ($n(T) \simeq [3\zeta(3)/\pi^2]T^3$ for $T \gtrsim m_\pi$). In the case when there is no threshold, the absorption rate also slowly increases with the J/ψ momentum since the average relative velocity of the J/ψ and the pion increases when p_T increases. However, this effect of the relative velocity is a very small effect. If indeed the J/ψ momentum is infinite the relative velocity is 1 and one has

$$\frac{1}{\theta} = \sigma \int \frac{d^3p'}{(2\pi)^3} f_\pi(E') \left[1 - \mathbf{v} \cdot \frac{\mathbf{p}'}{E'} \right] = \sigma n(T), \quad (2.13)$$

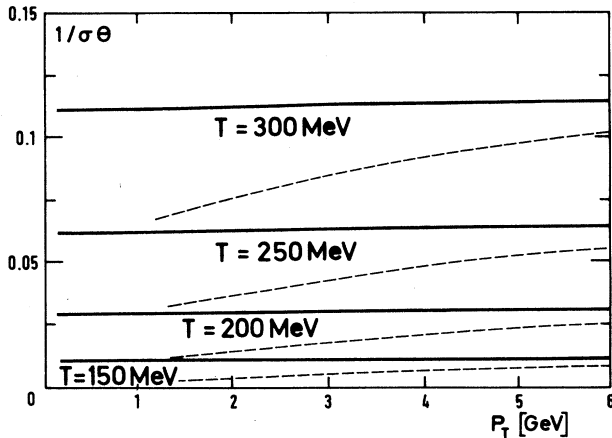


FIG. 1. The quantity $1/\sigma\theta$ as a function of the momentum p_T of the J/ψ , for a pion gas in thermal equilibrium. σ is the absorption cross section expressed in millibarns. θ is the collision time given by Eq. (2.12) and expressed in fm/c. The solid line corresponds to a constant cross section, while the dashed line includes the effect of the threshold for the reaction $\psi\pi \rightarrow D\bar{D}$.

where $n(T)$ is the fluid density at temperature T . On the other hand, when the J/ψ is at rest, that is, when $p_T = 0$, Eq. (2.12) gives

$$\frac{1}{\theta} = \sigma \int \frac{d^3p'}{(2\pi)^3} f_\pi(E') \frac{p'}{E'} = \sigma n(T) \langle v \rangle_T, \quad (2.14)$$

where $\langle v \rangle_T$ is the average thermal velocity of the pion. Comparing Eqs. (2.13) and (2.14) we see that the slight increase of the absorption rate with p_T in Fig. 1 is simply an effect of the π - ψ relative velocity. When $T = 100$ MeV, $\langle v \rangle_T = 0.862$ and when $T = 300$ MeV, $\langle v \rangle_T = 0.968$. Of course, the relative velocity is close to 1 because the pions behave nearly as massless particles for $T \gtrsim 100$ MeV. The effect of the variation of the relative velocity would be larger if more massive hadrons were considered. For example, with the ρ meson we would get $\langle v \rangle_T = 0.517$ when $T = 100$ MeV, and $\langle v \rangle_T = 0.752$ when $T = 300$ MeV. If the pion mass was strictly 0, the relative velocity would always be 1, and Eq. (2.13) would hold for any value of p_T . This means that in the zero-pion-mass limit, the collision time does not depend on p_T as long as there is no reaction threshold.

A much stronger dependence on the J/ψ momentum can be obtained if threshold effects are taken into account in the cross section. This is due to the fact that when the J/ψ momentum is low, very few pions have enough energy to reach the reaction threshold. When p_T goes to infinity, however, the ψ - π center-of-mass energy is always above threshold: thus the curves in Fig. 1 have the same asymptotic limit, given by Eq. (2.13). The threshold effect can be evaluated by considering the ratio of absorption rates $1/\theta$ with and without threshold, for a J/ψ at rest ($p_T = 0$). This ratio is 0.05 at $T = 100$ MeV, and 0.38 at $T = 200$ MeV, indicating that the threshold effect could be strong even for high temperatures.

B. J/ψ in an expanding pion gas

We now study the absorption of a J/ψ in a pion gas which undergoes a one-dimensional uniform expansion. We assume that the total entropy is conserved and therefore that the following law holds:¹⁶

$$s(T)t = s_0 t_0, \quad (2.15)$$

where $s(T)$ is the entropy density at temperature T , itself a function of time, and the index 0 refers to an arbitrary initial time. Equation (2.15) expresses the conservation of total entropy for the system whose volume increases like t . Let us recall that for massless particles, the entropy density is directly proportional to the particle number density n , $s = 3.6n$. We shall use this relation throughout this paper (strictly, it holds only for massless bosons).

Let us now study absorption of a J/ψ by this expanding pion gas. The integral over time t' in Eq. (2.3) can be replaced by an integral over the temperature, thanks to Eq. (2.15). A straightforward integration gives the fraction \mathcal{N} of J/ψ 's which remain after the temperature has dropped from T_0 to T :

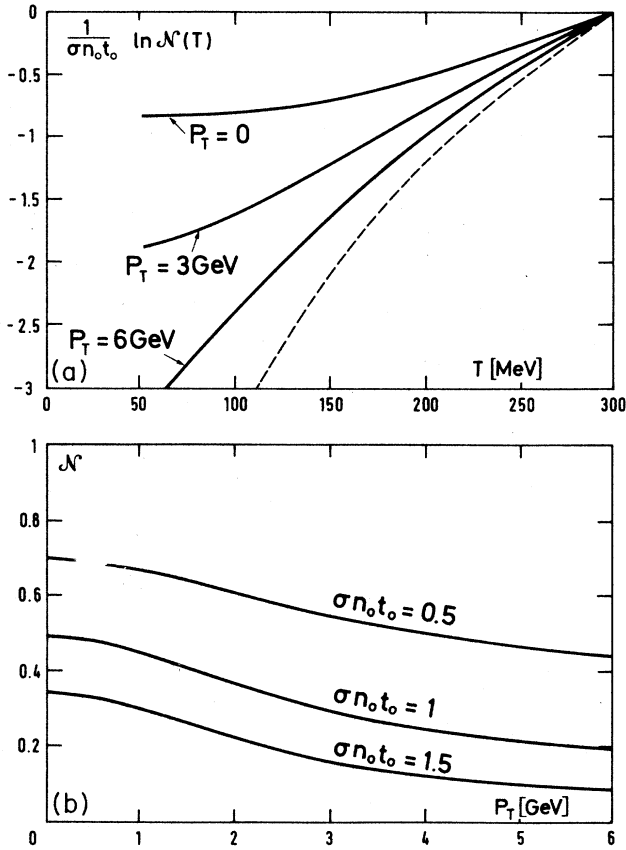


FIG. 2. (a) The quantity $(1/\sigma n_0 t_0) \ln \mathcal{N}(T)$ as a function of the temperature T . $\mathcal{N}(T)$ is chosen to be 1 when $T = 300$ MeV. The dashed curve corresponds to the zero pion mass limit [see Eq. (2.17)]. (b) The quantity $\mathcal{N}(T = 100 \text{ MeV})$ as a function of the momentum p_T of the J/ψ for several values of the dimensionless parameter $\sigma n_0 t_0$. As in (a), $\mathcal{N}(T = 300 \text{ MeV}) = 1$.

$$\ln \left[\frac{\mathcal{N}(T)}{\mathcal{N}(T_0)} \right] = -s_0 t_0 \int_{T_0}^T d \left[\frac{1}{s(T)} \right] \frac{1}{\theta(T)}, \quad (2.16)$$

where the collision time θ is defined in Eq. (2.11). Figure 2(a) shows how the absorption varies as a function of temperature for a few values of p_T , assuming a constant value for σ above a threshold which corresponds to the reaction $\psi\pi \rightarrow D\bar{D}$, as in Fig. 1. There is a strong dependence of \mathcal{N} on p_T : due to the reaction threshold, low-momentum J/ψ 's are only absorbed at high temperatures. For massless pions and in the limit $p_T \rightarrow \infty$, we can use Eq. (2.13) to estimate $\theta(T)$. Since both $n(T)$ and $s(T)$ are proportional to T^3 for massless pions, Eq. (2.16) becomes

$$\ln \left[\frac{\mathcal{N}(T)}{\mathcal{N}(T_0)} \right] = \frac{\sigma n(T_0) t_0}{3} \ln \left[\frac{T}{T_0} \right]. \quad (2.17)$$

This limit of zero pion mass and infinite p_T is the dashed

line in Fig. 2(a). Note that if there is no reaction threshold, \mathcal{N} does not depend on p_T so that the limit given by (2.17) holds in this case for any value of p_T .

A further illustration of the way a reaction threshold affects the survival probability is given in Fig. 2(b) which shows the fraction of J/ψ 's which remain at $T = 100$ MeV, as a function of their p_T and for typical values of the dimensionless parameter $\sigma n_0 t_0$. The shape of the curves reflects again the fact that the reaction threshold suppresses the absorption of low-momentum J/ψ 's.

We have chosen a specific reaction to estimate the effects of a threshold in the cross section. However, the conclusion we wish to draw from our calculation is a qualitative one which does not depend on the choice of this particular process (more quantitative studies taking into account other reactions have been considered in Refs. 8 and 10). We have seen that the existence of a threshold in the reaction cross section tends to decrease the absorption of low- p_T J/ψ 's. The effect of the relative velocity of the J/ψ with respect to the scatterers, which may be appreciable when the scatterers are massive particles, goes in the same direction. This behavior is opposite to that observed experimentally.⁵ For this reason, from now on, we shall ignore threshold effects and assume that the pions or more generally the scatterers are massless. Let us also remark that a reaction threshold can be defined without ambiguity whenever the interacting particles in the initial and the final states are well-defined objects; this may not be the case in the present problem.

If we let the temperature go to zero in Eq. (2.17), we see that \mathcal{N} goes to zero also: thus if the interaction region undergoes a longitudinal expansion only, all the J/ψ 's will eventually be absorbed. This is because, in this regime, the fluid density $n(T)$ decreases like $1/t$ [see Eq. (2.15)]. This result is unphysical since we know that the transverse expansion, which becomes important at times $t \approx R_0$, accelerates the dilution of the fluid: indeed, in a three-dimensional expansion $n(T)$ goes typically like $1/t^3$ and this is enough to allow the distribution function of J/ψ 's, $f(\mathbf{r}, \mathbf{p}_T, t)$, to converge in general to a nonzero value at large times. Along with the transverse expansion, finite-size effects must also be considered. Indeed, at times $t \gtrsim R_0$ a substantial fraction of the J/ψ 's having a velocity close to that of light will have escaped the interaction region, and this provides an extra cutoff on the absorption. These effects are studied in the next subsection.

C. Finite-size effects and the transverse expansion

Since we now have to cope with many physical effects, a few simplifying assumptions are necessary in order to solve Eq. (2.1). First, we assume a constant cross section σ (no reaction threshold) and massless scatterers in local thermal equilibrium. Then the J/ψ distribution is given by the solution of Eq. (2.6) which reads

$$f(\mathbf{r}, \mathbf{p}_T, t) = f_0(\mathbf{r} - \mathbf{v}t, \mathbf{p}_T) \exp \left[-\sigma \int_0^t n(\mathbf{x}, t') [1 - \mathbf{v} \cdot \mathbf{v}_f(\mathbf{x}, t')] dt' \right] \quad (2.18)$$

with $\mathbf{x} = \mathbf{r} - \mathbf{v}(t - t')$. Notice that the \mathbf{p}_T dependence appears in the geometric translation $\mathbf{v}(t - t')$ contained in \mathbf{x} , but also in the relativistic factor $(1 - \mathbf{v} \cdot \mathbf{v}_f)$.

We want to calculate the suppression factor \mathcal{A} , Eq. (2.4), using Eq. (2.18). Because it is difficult to calculate the integral over the J/ψ initial position \mathbf{r} , we are going to make a further simplifying assumption, namely that absorption is small for any of the J/ψ trajectories, which allows us to linearize the exponential in Eq. (2.18). We obtain then an approximate expression for the fraction of absorbed J/ψ 's:

$$\mathcal{A}_{\text{lin}}(\mathbf{p}_T) = \frac{\sigma \int d^2r f_0(\mathbf{r}, \mathbf{p}_T) \int_0^\infty dt n(\mathbf{x}, t) [1 - \mathbf{v} \cdot \mathbf{v}_f(\mathbf{x}, t)]}{\int d^2r f_0(\mathbf{r}, \mathbf{p}_T)}, \quad (2.19)$$

where $\mathbf{x} = \mathbf{r} + \mathbf{v}t$. For a central collision, n and v_f only depend on the distance r to the collision axis and \mathcal{A} depends only on p_T , the norm of \mathbf{p}_T . Let ϕ denote the angle between \mathbf{r} and \mathbf{v} , or equivalently between the fluid velocity and the J/ψ velocity; then Eq. (2.19) can be written in the form

$$\mathcal{A}_{\text{lin}}(p_T) = \int_0^\infty dr \int_0^\infty dt n(r, t) [g_1(r, vt) - vv_f(r, t)g_2(r, vt)], \quad (2.20)$$

where the integral over ϕ is contained in g_1 and g_2 , which are functions of r and of the distance $d = vt$ crossed by the J/ψ :

$$g_1(r, vt) = \frac{r \int_0^{2\pi} d\phi f_0(\mathbf{r} - \mathbf{v}t, \mathbf{p}_T)}{\int d^2r f_0(\mathbf{r}, \mathbf{p}_T)}, \quad (2.21)$$

$$g_2(r, vt) = \frac{r \int_0^{2\pi} d\phi f_0(\mathbf{r} - \mathbf{v}t, \mathbf{p}_T) \cos\phi}{\int d^2r f_0(\mathbf{r}, \mathbf{p}_T)}.$$

In our numerical estimates, we have taken the following expression for the initial J/ψ distribution function:³

$$f_0(r, p_T) = \frac{b+1}{\pi R_0^2} \left[1 - \frac{r^2}{R_0^2} \right]^b g(p_T), \quad (2.22)$$

where b is a free parameter which ranges from $\frac{1}{2}$ to 1 (see the Appendix). In Eq. (2.20), $n(r, t)$ and $\mathbf{v}_f(r, t)$ are computed using the hydrodynamical model developed in Ref. 17. We take for the initial fluid density $n(r, t_0)$ an expression similar to (2.22):

$$n(r, t_0) = (a+1)n_0 \left[1 - \frac{r^2}{R_0^2} \right]^a \quad (2.23)$$

and we assume that $v_f(r, t_0) = 0$.

Before we discuss our results, let us start by analyzing how the suppression factor \mathcal{A}_{lin} , given by Eq. (2.19), depends upon the parameters entering our problem. First of all, we note that \mathcal{A}_{lin} is obviously proportional to σ . It is also directly proportional to n_0 . Indeed, let n_0 be multiplied by a factor λ , which corresponds simply to a change in the initial temperature T_0 . Since our equation of state, which is that of an ideal gas of massless particles, does not contain any temperature scale, a change in T_0 does not induce any change in the hydrodynamic flow: v_f still takes the same values at any point, whereas n is multiplied by λ . Thus, \mathcal{A}_{lin} simply gets multiplied by λ , which proves our statement. Now let us keep n_0 constant and multiply both R_0 and t_0 by the same constant λ . In such a transformation, the distribution function f_0 , defined by Eq. (2.22), becomes $f'_0(r, p_T) = f_0(r/\lambda, p_T)/\lambda^2$, and similarly, the initial fluid density given by Eq. (2.23) becomes $n'(r, \lambda t_0) = n(r/\lambda, t_0)$. On the other hand, the

equations of hydrodynamics, when there are no dissipative terms, are invariant under a dilatation of space-time: ($r \rightarrow \lambda r$, $t \rightarrow \lambda t$). It follows, for example, that the density n' and the fluid velocity v'_f corresponding to the new (scaled) boundary conditions are given by $n'(r, t) = n(r/\lambda, t/\lambda)$ and $v'_f(r, t) = v_f(r/\lambda, t/\lambda)$. Using this scaled solution in Eq. (2.19) and performing the change of variable $r/\lambda = r'$, $t/\lambda = t'$, we find that, in the transformation considered, $\mathcal{A}_{\text{lin}} \rightarrow \lambda \mathcal{A}_{\text{lin}}$. We conclude that $\mathcal{A}_{\text{lin}}(p_T)$ may be written as the product of $\sigma n_0 t_0$ and a universal function of t_0/R_0 and p_T (as well as of the parameters a and b of the initial distribution):

$$\mathcal{A}_{\text{lin}}(p_T) = \sigma n_0 t_0 h \left[\frac{t_0}{R_0}, p_T \right]. \quad (2.24)$$

In Fig. 3 we show the behavior of $h(t_0/R_0, p_T)$ as a function of p_T , for a few values of t_0/R_0 . The absorption is decreasing with increasing p_T and saturates when $p_T \gtrsim 3$ GeV. This saturation is easily understood since p_T appears only through \mathbf{v} in Eq. (2.19) and $\mathcal{A}_{\text{lin}}(p_T)$ quickly converges when $p_T \gtrsim 3$ GeV to a nonzero limit which corresponds to $v = 1$. Thus, there is a residual absorption,

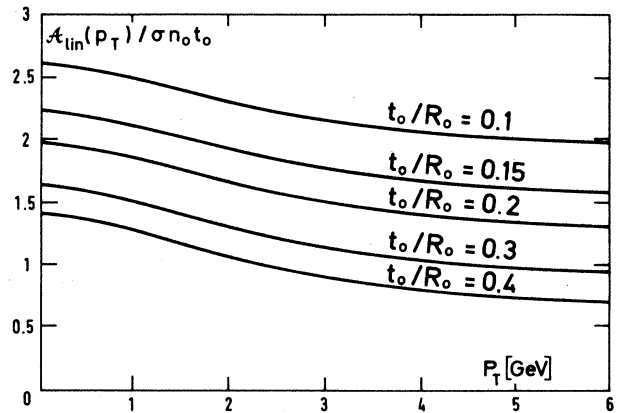


FIG. 3. The absorption factor $\mathcal{A}_{\text{lin}}(p_T)$ in units of the dimensionless parameter $\sigma n_0 t_0$ as a function of the J/ψ momentum p_T , and for various values of t_0/R_0 . t_0 is the time at which matter appears in the central rapidity region and starts to expand; it is also the time at which the absorption starts.

even for high p_T . We also notice that the absorption increases when t_0/R_0 decreases, which follows simply from the fact that t_0 is the time at which the absorption starts. Note that the curves in Fig. 3 are roughly parallel. This can be easily understood in the following way: we know from a previous study¹⁸ that hydrodynamic flows do not depend on t_0 provided $t_0 \ll R_0$ and $n_0 t_0$ is held constant. Thus, the increase in $h(t_0/R_0, p_T)$ between two values of t_0 , t_{01} ($\ll R_0$) and $t_{02} < t_{01}$, simply comes from the absorption between $t = t_{02}$ and $t = t_{01}$. In order to evaluate this contribution, we make use of Eq. (2.19) again. Since the fluid transverse velocity is small at early times, we may set $v_f \simeq 0$; furthermore, between t_{01} and t_{02} , the J/ψ 's travel a distance which is small compared to R_0 . Thus, we are back to the situation discussed in Sec. II B where transverse expansion and finite geometry were ignored. The integral over t can be carried out using the relation $t = t_0 n(r, t_0)/n(r, t)$. The result is

$$\mathcal{A}_{\text{lin}}(p_T) = \sigma \bar{n}_0 t_0 \ln \frac{t_{01}}{t_{02}} \quad (t_{02} < t < t_{01}), \quad (2.25)$$

where

$$\bar{n}_0 \equiv \frac{\int d^2r f_0(\mathbf{r}) n(\mathbf{r}, t_0)}{\int d^2r f_0(\mathbf{r})} \quad (2.26)$$

is the mean value of $n(\mathbf{r}, t_0)$ over \mathbf{r} , weighted by the distribution function f_0 of $c\bar{c}$ pairs. For example, with the initial distributions given by Eqs. (2.22) and (2.23), we get

$$\bar{n}_0 = n_0 \frac{(a+1)(b+1)}{a+b+1}. \quad (2.27)$$

The logarithmic behavior implied by Eq. (2.25) is clearly visible in Fig. 3. Equation (2.25) expresses the fact that absorption at early times is independent of p_T . Indeed, the initial distribution $f_0(\mathbf{r})$ is assumed to be independent of p_T ; and from Sec. II B, we know that absorption on massless particles does not depend on p_T if there is no reaction threshold. This point is further illustrated in Fig. 4 which shows the results obtained by switching on the

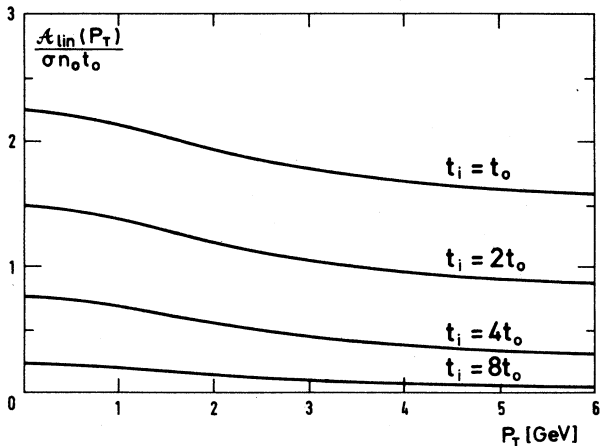


FIG. 4. Same as Fig. 3, but here the absorption is allowed to start at various times $t_i \geq t_0$; for all these curves, $t_0/R_0 = 0.15$.

absorption at various times $t_i > t_0$, t_0 being as before the time at which the fluid starts to expand. We see that the curves for $t_i = t_0$ and $t_i = 2t_0$ are parallel, which expresses that the absorption between t_0 and $2t_0$ is independent of p_T . Most of the p_T dependence comes from the absorption at $t > 4t_0$, and finds its origin in effects related to the transverse expansion and the finite size of the system.

In the preceding calculation, we have assumed that the absorption is small; this has allowed us to give a full treatment of geometry and transverse expansion. However, if we are to believe experimental results, J/ψ suppression may exceed 50% at low p_T . Thus, it is important to have an estimate of nonlinear terms in Eq. (2.18) and as a simple approximation we shall use

$$\mathcal{N}_{\text{app}}(p_T) = \exp[-\mathcal{A}_{\text{lin}}(p_T)], \quad (2.28)$$

which is to be compared to the exact value obtained from Eqs. (2.4) and (2.18). Equation (2.28) means that we take the exponential of the average over the J/ψ initial positions in place of the average of the exponential which would correspond to the exact calculation. Since the exponential is a convex function, $\mathcal{N}_{\text{app}}(p_T) \leq \mathcal{N}(p_T)$. That is, our approximation overestimates the absorption. Equality would actually be obtained if the probability for the J/ψ to be absorbed was the same along all the possible trajectories. The validity of our approximation can in fact be checked easily when $p_T = 0$, in which case the exact value is

$$\mathcal{N}(p_T = 0) = \frac{\int d^2r f_0(\mathbf{r}) \exp\left[-\sigma \int_0^\infty n(\mathbf{r}, t) dt\right]}{\int d^2r f_0(\mathbf{r})}. \quad (2.29)$$

This value is shown in Fig. 5, together with the approximation given by (2.28). One sees that the error, which reflects the fact that the ψ trajectories are not all equivalent to each other, is only a few percent in absolute magnitude, and (2.28) is therefore excellent for all practical purposes.

We can now present an approximate formula which ac-

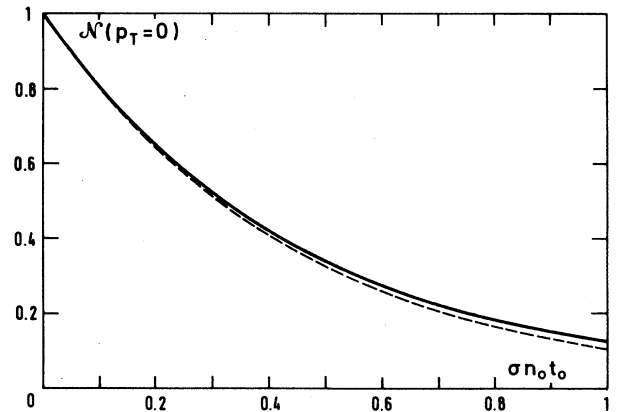


FIG. 5. Fraction of surviving J/ψ 's with zero momentum as the function of the dimensionless parameter $\sigma n_0 t_0$. The solid line corresponds to the exact calculation (2.29). The dashed line is the linear approximation (2.28). As in Fig. 4, $t_0/R_0 = 0.15$.

counts in a simple way for the combined effects of finite size and transverse expansion. This formula will be useful in the next section where we shall be dealing with the full complexity of nonzero impact-parameter collisions. It is obtained by assuming that the J/ψ interacts after time t_0 with a longitudinally expanding fluid, from which it escapes freely at a freeze-out time t_f . This freeze-out time t_f , which depends on p_T , acts as an effective cutoff of the absorption. From Eq. (2.25) one gets

$$\mathcal{A}_{\text{lin}}(p_T) = \sigma \bar{n}_0 t_0 \ln \left[\frac{t_f}{t_0} \right] \quad (2.30)$$

with \bar{n}_0 given by Eq. (2.26). We use the numerically determined value of $\mathcal{A}_{\text{lin}}(p_T)$ displayed in Fig. 3 to determine the value which should be taken for $t_f(p_T)$ if one wants Eq. (2.30) to give the exact result. For example, for the value $t_0/R_0 = 0.15$, which is physically reasonable (see Sec. IV), we find $t_f(p_T=0) \simeq 1.1R_0$ and $t_f(p_T=6 \text{ GeV}) \simeq 0.6R_0$. These values are somewhat lower than those used in previous works based on a similar approximate formula.⁹ Figure 6 displays t_f/R_0 as a function of t_0/R_0 , for a few values of p_T . It is another way to present the results displayed in Fig. 3: for instance, the fact that the curves for different t_0/R_0 are roughly parallel in Fig. 3 expresses that the dependence of t_f on t_0 is rather weak, as can be seen in Fig. 6, and thus the variation in \mathcal{A}_{lin} with t_0 comes mainly from its explicit dependence on t_0 in Eq. (2.30) rather than from $t_f(t_0)$.

We now come to our final result. With \mathcal{A}_{lin} given by Eq. (2.30) we get from (2.28) the following expression for the fraction of J/ψ 's surviving inelastic interactions with the expanding fluid:

$$\mathcal{N}(p_T) \simeq \left[\frac{t_0}{t_f} \right]^{\sigma \bar{n}_0 t_0}, \quad (2.31)$$

where \bar{n}_0 is given by Eq. (2.26) and the dependence on p_T is hidden in t_f . From Fig. 6 one sees that t_f decreases by some 40% when p_T goes from zero to infinity. Note that

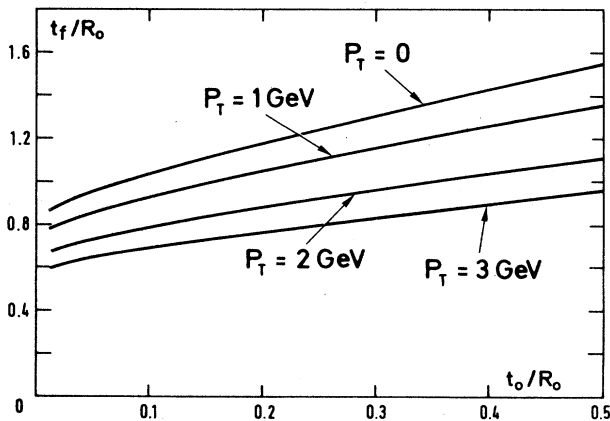


FIG. 6. The freeze-out time t_f for various values of the J/ψ transverse momentum as a function of the initial time t_0 at which matter is formed in the central region and absorption starts [see Eq. (2.31)].

absorption does not stop for large p_T , in contrast with the model studied in the next section. The variation of $\mathcal{N}(p_T)$ with the dimensionless parameter $\sigma n_0 t_0$ is illustrated in Fig. 7 for two typical values of t_0/t_f corresponding to a central oxygen-uranium collision and a central oxygen-copper collision (see Sec. IV).

III. J/ψ SUPPRESSION BY A QUARK-GLUON PLASMA

Let us start by recalling the basic features of the models for J/ψ suppression which invoke the Debye screening of the $c\bar{c}$ potential at high temperature.¹⁻⁴ This is most conveniently done by looking at the space-time diagram of Fig. 8. As discussed at the beginning of Sec. II, the $c\bar{c}$ pair is created at time $t=0$. Its center of mass then evolves along a straight line, while at the same time the quark and the antiquark separate with a velocity characteristic of their relative motion in the J/ψ bound state. In a frame where the center of mass of the $c\bar{c}$ pair is at rest, it takes a time τ_ψ before the separation reaches the size of the J/ψ bound state. In the laboratory frame, this time is dilated by a factor which depends on the momentum p_T of the pair:

$$t_\psi = \tau_\psi \left[1 + \frac{p_T^2}{M^2} \right]^{1/2} \quad (3.1)$$

and in the space-time diagram of Fig. 8 the J/ψ s are formed on the hyperbola of constant $\tau_\psi = \sqrt{t^2 - (r-r_0)^2}$.

At the same time as the charm-quark pair is propagating through the system, the plasma is cooling due to its rapid expansion. The Debye screening will inhibit the formation of the resonance whenever the temperature at the formation point is higher than some characteristic temperature T_D . This leads to the consideration of the isotherm $T=T_D$ which is drawn in the diagram. The predictions of our model are simply obtained by counting

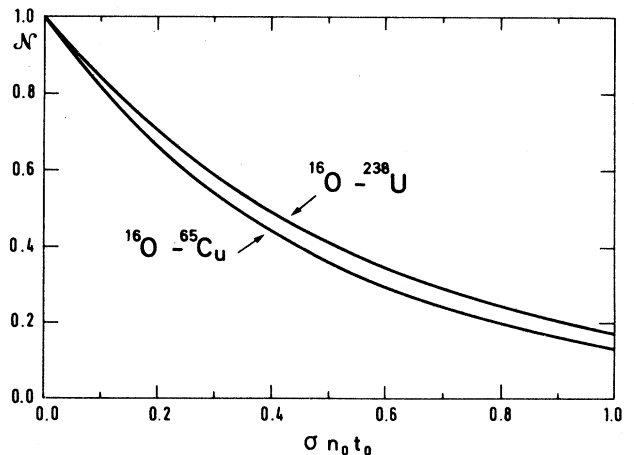


FIG. 7. The fraction of surviving J/ψ after absorption by a hot pion gas, as a function of the dimensionless parameter $\sigma n_0 t_0$. The upper curve corresponds to a central oxygen-uranium collision for which we take $t_0/R_0 = 0.17$, the lower curve to a central oxygen-copper collision for which $t_0/R_0 = 0.13$ (see Sec. IV, Table I).

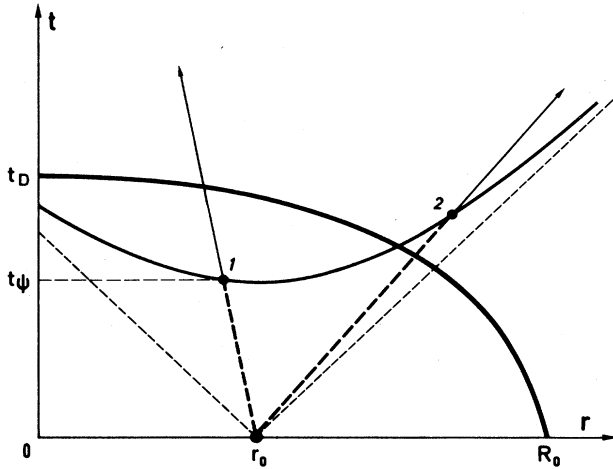


FIG. 8. Space-time diagram illustrating the various factors which enter the calculation of the J/ψ suppression based on Debye screening. The line which goes from $(t=0, r=R_0)$ to $(t_D, 0)$ is the isotherm $T(r,t)=T_D$. The point $(0, r_0)$ is the point where the $c\bar{c}$ pair is produced. Dashed lines indicate the light cone of the center of mass of the pair. Also indicated is the hyperbola of constant proper time $\sqrt{t^2 - (r - r_0)^2} = \tau_\psi$, where τ_ψ is the J/ψ formation time. The $c\bar{c}$ pair going through the point labeled (1) will not give birth to a J/ψ , whereas the one going through point labeled (2) will.

as produced J/ψ 's only those which are formed outside the isotherm. Thus, the model establishes a correlation between the momentum distribution of the produced J/ψ 's and the space-time evolution of the plasma.

With an initial density profile of the plasma given by Eq. (2.23), and taking into account only the longitudinal expansion of the plasma, one obtains a simple parameterization of the isotherms in the (r,t) plane. These are circles with radius

$$R(t) = R_0 [1 - (t/t_D)^{1/a}]^{1/2}, \quad (3.2)$$

where t_D is the time at which the isotherm reaches the collision axis, that is the time at which all the plasma has cooled down to a temperature less than or equal to T_D . This time t_D , to which we shall loosely refer as the lifetime of the plasma, is given by

$$t_D = \frac{s_0 t_0}{s_D} = \frac{n_0 t_0}{n_D}. \quad (3.3)$$

A characteristic feature of the model is its prediction concerning the dependence of the J/ψ suppression on the J/ψ momentum p_T . In particular a simple formula was obtained in Ref. 3 for the number of produced J/ψ 's as a function of their p_T :

$$\mathcal{N} = \left[\frac{t_\psi}{t_D} \right]^{(1+b)/a}, \quad (3.4)$$

where t_ψ is related to p_T by (3.1), and a, b are the parameters entering the distributions (2.23), (2.22). This number \mathcal{N} cannot be greater than 1 so that there exists a maximum value of p_T , p_T^{\max} , given by

$$p_T^{\max} = M \left[\left(\frac{t_D}{\tau_\psi} \right)^2 - 1 \right]^{1/2} \quad (3.5)$$

beyond which no suppression takes place. Actually the formula (3.4) only holds in cases where the plasma lives for a time short compared to the average transit time t_1 of a J/ψ in the system, $t_1 \sim (8R_0/3\pi)[1 + (M/p_T)^2]^{1/2}$. If this is not the case, a maximum transverse momentum still exists and is obtained by equating t_1 with t_ψ ; this gives

$$p_T^{\max} = M \frac{8}{3\pi} \frac{R_0}{\tau_\psi}. \quad (3.6)$$

This value reflects a finite-size effect: a J/ψ with a large p_T escapes the interaction region before it is formed, and it is not affected by the plasma. The value of p_T^{\max} deduced from (3.6), which corresponds essentially to that found in the original work by Karsch and Petronzio,² is in general much larger than the one predicted by Eq. (3.5). In the rest of this work, we shall only consider situations where $t_D < t_1$ and shall consequently ignore finite-size effects when discussing J/ψ suppression by a quark-gluon plasma.

Let us now turn to the dependence of the results upon the initial conditions in the plasma. To make things simple, we shall consider the distribution (2.23) with $a \rightarrow 0$, corresponding to a uniform entropy density of the plasma. Then from Eq. (3.4) one gets

$$\mathcal{N} = \begin{cases} 0 & \text{if } t_\psi < t_D, \\ 1 & \text{if } t_\psi > t_D. \end{cases} \quad (3.7)$$

The critical value of t_ψ at which suppression sets in is then given by

$$t_\psi = t_D = \frac{n_0 t_0}{n_D}, \quad (3.8)$$

which reveals that $t_\psi n_D$ is the important critical parameter. If indeed $n_0 t_0 > n_D t_\psi$, then $t_D > t_\psi$ and there will be suppression. If $n_0 t_0 < n_D t_\psi$ there will be no suppression. Note that $n_D t_\psi$ depends upon the momentum of the ψ . If $n_0 t_0 < n_D \tau_\psi$, there will be no suppression for any p_T , thus $\mathcal{N} = 1$. If, on the contrary, $n_0 t_0 > n_D \tau_\psi$, the pairs with momentum $p_T < p_T^{\max}$ will be suppressed, with p_T^{\max} given by Eq. (3.5), or equivalently by

$$1 + \left[\frac{p_T^{\max}}{M} \right]^2 = \left[\frac{n_0 t_0}{n_D \tau_\psi} \right]^2. \quad (3.9)$$

In order to estimate the total amount of suppression, one needs therefore to know the p_T distribution of the $c\bar{c}$ pairs which we take of the form

$$g(p_T) \propto p_T \exp(-p_T/p_{T0}). \quad (3.10)$$

This distribution is compatible with the experimental data from which one can extract $p_{T0} \approx 570$ MeV/c (Ref. 5). Integrating over p_T , one then finds

$$\mathcal{N} = \left[1 + \frac{p_T^{\max}}{P_{T0}} \right] \exp \left[-\frac{p_T^{\max}}{P_{T0}} \right]. \quad (3.11)$$

The variation of \mathcal{N} as a function of the dimensionless parameter $n_0 t_0 / n_D \tau_\psi$ is a universal curve given in Fig. 9.

The parameter $n_D \tau_\psi$ depends in principle on the type of resonance one is considering. Here we refer constantly to the J/ψ but similar considerations apply as well to the ψ' or to the χ , for example. The various estimates of these parameters which have been attempted so far leave us with a large uncertainty. The minimum Debye radius below which no bound state can exist is obtained from the solution of the Schrödinger equation for the resonance and depends on the specific form of the $c\bar{c}$ potential. This minimum Debye radius is related to the temperature T_D which can, in principle, be obtained from lattice gauge calculations.¹⁹ Thus n_D , which is proportional to T_D^3 , is subject to the uncertainties in both the $c\bar{c}$ potential and lattice gauge calculations. Furthermore, the formation time is not known either with a good precision. As a result, we are not able to make quantitative predictions for the values of $n_D \tau_\psi$ corresponding to different resonances.

Let us now summarize the main qualitative features of the two mechanisms which we have studied in Secs. II and III. Both of them predict a decrease of the total J/ψ yield as a function of the control parameter of the problem which in both cases appears to be the number of particles per unit area $n_0 t_0 \propto A^{-2/3} dN/dy$. However, this is a smooth and regular decrease for the absorption process, while Debye screening sets in only when $n_0 t_0$ exceeds a certain value. The most dramatic difference between the two mechanisms is the p_T dependence. There is a cutoff in the plasma model, while the absorption picture leads to a very weak dependence on p_T , the absorption taking place for arbitrarily large p_T . Let us mention that recent attempts to explain the J/ψ suppression in terms of an

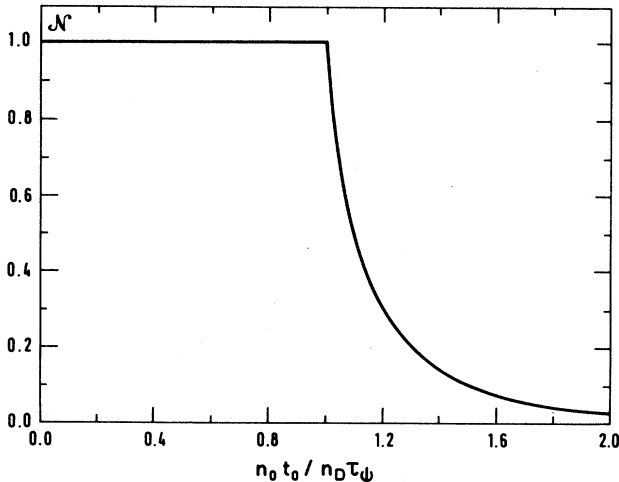


FIG. 9. The fraction of produced J/ψ 's in the presence of a quark-gluon plasma, as a function of the parameter ratio $n_0 t_0 / n_D \tau_\psi$. As explained in the text, the plasma suppression sets in only when $n_0 t_0 \geq n_D \tau_\psi$.

absorption mechanism have obtained a rather strong p_T dependence in their results.^{8,9} This is simply because they include in their calculation a formation time for the J/ψ . The effect of the formation time is easy to understand. In the plasma model, a J/ψ with a large p_T is formed after the plasma has cooled down to a low enough temperature. In the absorption model, a J/ψ with a large p_T starts to be absorbed only when the density is low and has therefore little absorptive power. However, in this later case, the use of a formation time seems to us very little justified, for reasons which we explained in Sec. II.

IV. RESULTS AND COMPARISON WITH EXPERIMENT

The NA38 Collaboration at CERN (Ref. 5) measures the dimuons which are produced in nucleus-nucleus collisions, with a mass of the order of the J/ψ mass. Continuum $\mu^+ \mu^-$ pairs which are produced directly, for instance, in a Drell-Yan process, interact weakly after they are formed, and are not expected to disappear. On the contrary, a resonance such as the J/ψ , which also decays into $\mu^+ \mu^-$, may be destroyed by any of the two suppression mechanisms described in the previous section. In order to provide a measure of the suppression, one calculates the ratio S of the number of muon pairs coming from J/ψ decays to the number of continuum dimuons. This is done for several bunches of events classified according to the total transverse energy produced in the collision. It is found that the ratio S decreases with increasing E_T , the suppression being enhanced at low p_T .

In order to compare our results with experimental data, we need a model for the space-time distribution of J/ψ 's and pions, as well as its relation to transverse energy. We shall use the fact that the transverse energy, as well as the multiplicity density in the central rapidity region, are proportional to the average number of participant nucleons.^{20,21} We recall in the Appendix how these can be related to the impact parameter in a simple geometrical model. As for the initial distribution of $c\bar{c}$ pairs, we assume that it is proportional to the number of individual nucleon-nucleon collisions. Details are given in the Appendix.

Let us now discuss how the parameters of the model have been adjusted. In both models, we have one unknown parameter: the inelastic cross section σ in one case, and the quantity $n_D \tau_\psi$ in the other case. The probability to produce a J/ψ is proportional to the probability to produce a $c\bar{c}$ pair multiplied by the survival probability $\mathcal{N}(b)$ defined in the previous sections. We shall explain later how we calculate \mathcal{N} as a function of the impact parameter. As said before, we assume that the probability to produce a $c\bar{c}$ pair is proportional to $T_{AB}(b)$, that is to the number of nucleon-nucleon collisions at impact parameter b (see the Appendix). Then we have

$$\frac{d\sigma_{AB \rightarrow \psi}}{dE_T} = \sigma_{NN \rightarrow \psi} T_{AB}(b) \mathcal{N}(b) \frac{2\pi b db}{dE_T}. \quad (4.1)$$

We assume that the number of continuum events may be evaluated from Eq. (4.1) with $\mathcal{N}(b)$ set equal to 1. Let

then S_1 be the ratio of J/ψ over continuum muon pairs in a low-transverse-energy bin, say $E_1 < E_T < E'_1$ and S_2 the same ratio in a high-transverse-energy bin, say $E_2 < E_T < E'_2$; then, provided the two bins contain the same numbers of continuum events, we obtain an experimental measure of J/ψ suppression which can be compared to the calculated value

$$\frac{S_2}{S_1} = \frac{\int_{E_2}^{E'_2} \frac{d\sigma_\psi}{dE_T} dE_T}{\int_{E_1}^{E'_1} \frac{d\sigma_\psi}{dE_T} dE_T}. \quad (4.2)$$

The crudest way to measure J/ψ suppression is to take only two bins: the events are separated in two sets, one containing the low-transverse-energy events (smaller than some value E_{T0}), and the other the high-transverse-energy (bigger than E_{T0}) events. We have chosen to adjust the parameters in our model in such a way that the corresponding ratio S_2/S_1 , Eq. (4.2), falls in the range 70–75 % for 200-GeV/nucleon oxygen-uranium collisions, as indicated by NA38 data.⁵ This leads us to the values $\sigma \simeq 1.5$ mb and $n_D \tau_\psi \simeq 5.5$ fm⁻². If the formation time takes the value $\tau_\psi = 0.7$ fm/c, this value of $n_D \tau_\psi$ corresponds, for a plasma made of u and d quarks, to a temperature $T_D \simeq 240$ MeV above which the J/ψ cannot be formed.

In order to evaluate the amount of J/ψ suppression induced by inelastic scattering, we use the approximate formula (2.31) derived at the end of Sec. II. This formula strictly applies to central collisions. However, we shall use it also for nonzero impact parameter, taking advantage of our understanding of central collisions to propose reasonable estimates of the various quantities which enter this formula.

The first thing we need is an estimate of the time t_0 at which the $c\bar{c}$ system starts to interact with the surrounding matter. As mentioned at the beginning of Sec. II we choose for t_0 half the time it takes for the nuclei to cross each other; for the collisions of two nuclei with radii R_A and R_B , at impact parameter b , we take

$$t_0 = \frac{1}{2\gamma_{c.m.}} [(R_A + R_B)^2 - b^2]^{1/2}, \quad (4.3)$$

where $\gamma_{c.m.}$ is the γ factor of the nucleons in the center-of-mass frame of a colliding nucleon-nucleon pair ($\gamma_{c.m.} \simeq 10$ at 200 GeV/nucleon). It was found in Sec. II C that for a central collision, the quantity t_0/R_0 is an important parameter. For a collision of nonidentical nu-

clei R_0 is understood as being the smallest of R_A and R_B . Typical values of t_0/R_0 for $b=0$ are listed in Table I.

Next, we must estimate the freeze-out time t_f at which the J/ψ ceases to interact with the surrounding matter. As explained at the end of Sec. II, t_f incorporates all the effects of finite size and transverse expansion and is proportional to the radius of the region of interaction. We distinguish two cases ($R_A > R_B$): $b < R_A - R_B$, the collision is fairly central and the interaction region is a disk with radius R_B , and we take the same value for t_f as for a central collision; $b > R_A - R_B$, the region of interaction is no more circular [see Fig. 16(b) below] and the time required for the transverse expansion to reach the middle of the interaction region is of the order of $(R_A + R_B - b)/2$. In this case, we take for t_f the value appropriate for a central collision, multiplied by the factor $(R_A + R_B - b)/2R_B$. In order to determine the freeze-out time t_f for $b=0$, we refer to Fig. 6 in Sec. II. There it can be seen that for $p_T=1$ GeV, which is roughly the mean value of p_T , we have $t_f \simeq R_0$ for all values of t_0/R_0 between 0.1 and 0.2; this is the value that we shall take.

With these estimates of t_f and t_0 , we are ready to compute \mathcal{N} from Eq. (2.31). We compute \bar{n}_0 [Eq. (2.26)] using the distributions derived in the Appendix. The resulting \mathcal{N} is displayed in Fig. 10 as a function of $(\sigma/S_{\text{eff}})dN/dy$. The present estimate takes into account the fact that for a peripheral collision, it takes less time for the transverse expansion to cool the system than for a central one. This effect is partly balanced by the decrease of t_0 with increasing impact parameter. The spatial inhomogeneities of the initial distribution of $c\bar{c}$ pairs and pions represent only a correction of a few percent which enhances absorption for central collisions. In fact, a crude approximation consists in ignoring the variation with b of t_0/t_f and in replacing $\bar{n}_0 t_0$ by $(1/S_{\text{eff}})dN/dy$. This yields the dashed lines in Fig. 10. Note that there is a turning point in the solid curve of Fig. 10(b); this is due to the fact that $(\sigma/S_{\text{eff}})dN/dy$ is not a monotonous function of b for a lead on lead collision, and thus there may be two values of b that give the same value of $(\sigma/S_{\text{eff}})dN/dy$. The latter quantity reaches its maximum value at an impact parameter $b=3.6$ fm and is there 20% higher than for an oxygen-uranium collision [see the Appendix and Fig. 17(b)]. Note that the parameter $(\sigma/S_{\text{eff}})dN/dy$ does not absorb the full A dependence of \mathcal{N} and the curves in Fig. 10 still depend upon which collision is involved. In particular there is more absorption, i.e., \mathcal{N} is lower, in Pb-Pb collision than in O-U collision because $t_0/t_f=0.1$ for Pb-Pb instead of 0.17 for O-U.

Figure 11 displays the variation of \mathcal{N} with p_T for an oxygen-uranium collision and for two values of the impact parameter. We see that the behavior of \mathcal{N} with p_T is the same for a peripheral collision with $b=6$ fm as for a central collision. In particular, the ratio $\mathcal{N}(b=0)/\mathcal{N}(b=6 \text{ fm})$ will be almost independent of p_T .

Let us now study the J/ψ suppression due to Debye screening. Here, it is a good approximation³ to ignore effects of finite size and of transverse expansion. Assuming that no J/ψ is going to be formed at point \mathbf{r} if $n(\mathbf{r}, t_0)t_0 > n_D t_\psi$, with $t_\psi = \tau_\psi [1 + (p_T/m)^2]^{1/2}$, we obtain

TABLE I. Values of t_0/R_0 used in our calculations for central collisions.

	t_0/R_0
¹⁶ O- ²³⁸ U	0.17
³² S- ²³⁸ U	0.15
¹⁶ O- ⁶⁵ Cu	0.13
²⁰⁸ Pb- ²⁰⁸ Pb	0.10

$$\mathcal{N}(p_T) = 1 - \frac{\int_{H'} d^2r f_0(\mathbf{r})}{\int d^2r f_0(\mathbf{r})}, \quad (4.4)$$

where the integral in the numerator is carried over the region H' where $n(\mathbf{r}, t_0)t_0 > n_D t_\psi$. In writing Eq. (4.4), we have also assumed that $f_0(\mathbf{r} - \mathbf{v}t_\psi) \simeq f_0(\mathbf{r})$, in line with the fact that we ignore finite-size effects. The fraction $\mathcal{N}(p_T)$ can be easily integrated over p_T :

$$\mathcal{N} = 1 - \frac{\int_H f_0(\mathbf{r}) \left[1 + \frac{p_T^{\max}}{P_{T0}} \right] \exp \left[-\frac{p_T^{\max}}{P_{T0}} \right] d^2r}{\int d^2r f_0(\mathbf{r})}, \quad (4.5)$$

where

$$p_T^{\max} = M \left[\frac{n(\mathbf{r}, t_0)t_0}{n_D \tau_\psi} - 1 \right]^{1/2}$$

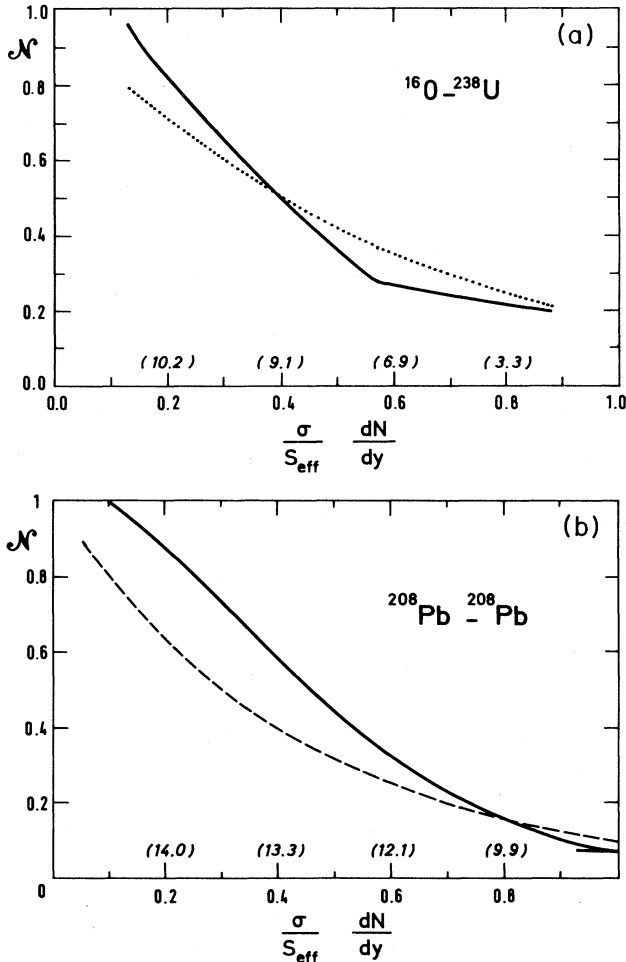


FIG. 10. The fraction of surviving J/ψ 's after absorption by the pion gas formed in a nucleus-nucleus collision, as a function of the control parameter $(\sigma/S_{\text{eff}})dN/dy$; the dashed line is the crude estimate given in (2.31), and displayed in Fig. 7. (a) Oxygen-uranium collision; (b) lead-lead collision. In both cases we have taken the value $\sigma=1.5$ mb. The numbers in parentheses are the values of the impact parameter b in fm.

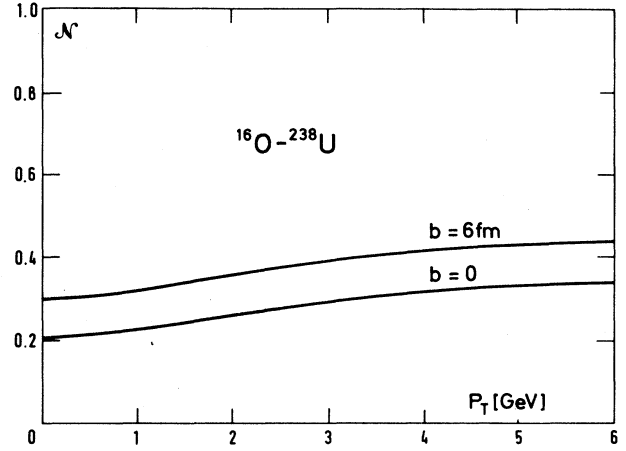


FIG. 11. p_T dependence of J/ψ absorption by a pion gas, in the case of an oxygen-uranium collision, for two values of the impact parameter: $b=0$ corresponds to a central collision, that is to a maximum suppression; $b=6$ fm is a peripheral collision. As in Fig. 10, $\sigma=1.5$ mb.

is the maximum transverse momentum for which the formation of the resonance is inhibited, and H is the region where $n(\mathbf{r}, t_0)t_0 > n_D \tau_\psi$.

In Fig. 12, numerical results are presented as a function of $1/(n_D \tau_\psi S_{\text{eff}})dN/dy$. These are compared with the result of a simpler approximation in which one ignores inhomogeneities of the initial distribution; then \mathcal{N} is given by Eq. (3.11) and the parameter $n_0 t_0$ is set equal to $(1/S_{\text{eff}})dN/dy$ (dashed lines in Fig. 12). In the case of a central oxygen-uranium collision [Fig. 12(a)], the dimensionless parameter $1/(n_D \tau_\psi S_{\text{eff}})dN/dy$ is only slightly above 1 which is the critical value for the J/ψ suppression to set in. As a consequence, the inhomogeneities of the initial distribution, which are taken into account in Eq. (4.4), play an important role. In a lead-lead collision, the parameter $1/(n_D \tau_\psi S_{\text{eff}})dN/dy$ has a maximum value which is 20% higher than in an oxygen-uranium collision. Although this may seem to be weak, it is not since the typical variation of \mathcal{N} with this parameter, displayed in Fig. 9, is very steep. Indeed, we find some 75% maximum suppression for lead-lead, instead of 50% for oxygen-uranium. Note that the solid curve in Fig. 12(b) has a turning point, for the same reason as in Fig. 10(b).

The p_T dependence of the suppression induced by a quark-gluon plasma in an oxygen-uranium collision is displayed in Fig. 13 for two values of the impact parameter. If there is large suppression at low p_T for a central collision, we see that there is hardly any suppression at all for a peripheral collision with $b=6$ fm. This behavior is very different from that obtained with the absorption model. In particular there is a maximum value beyond which the suppression disappears.

Let us now discuss our results in terms of their dependence on the transverse energy of the collision or equivalently on the number of participants. Figure 14 displays, for the absorption model, the dependence of the surviving fraction of J/ψ 's on the number of partici-

pants. We see that absorption is already important for peripheral collisions, and saturates for central collisions. An indication on how absorption depends on the transverse momentum of the pair is also shown in the same figure: the p_T dependence of the effect does not exceed 20% even for very central collisions, and furthermore has a very flat variation with E_T . Corresponding results for the plasma model are displayed in Fig. 15. Let us first look at Fig. 15(a). The variation of \mathcal{N} is very different from that seen in Fig. 14(a): indeed, for peripheral collisions, the plasma is not hot enough and there is no suppression at all. On the other hand, suppression is very important for central collisions. The p_T dependence is also very different, as was expected from the general dis-

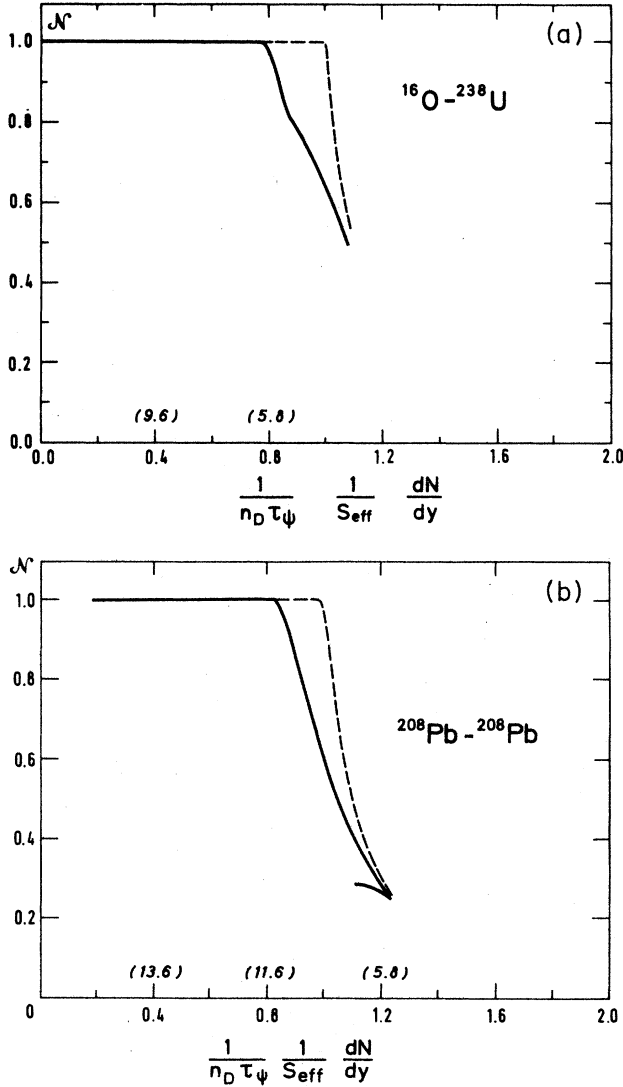


FIG. 12. The fraction of J/ψ 's remaining after interaction with a quark-gluon plasma, as a function of the control parameter $(1/n_D \tau_\psi S_{\text{eff}}) dN/dy$; the dashed line is the universal curve shown in Fig. 7. (a) Oxygen-uranium collision; (b) lead-lead collision. For both, we have taken $n_D \tau_\psi = 5.5 \text{ fm}^{-2}$. The numbers in parentheses are the values of the impact parameter b in fm.

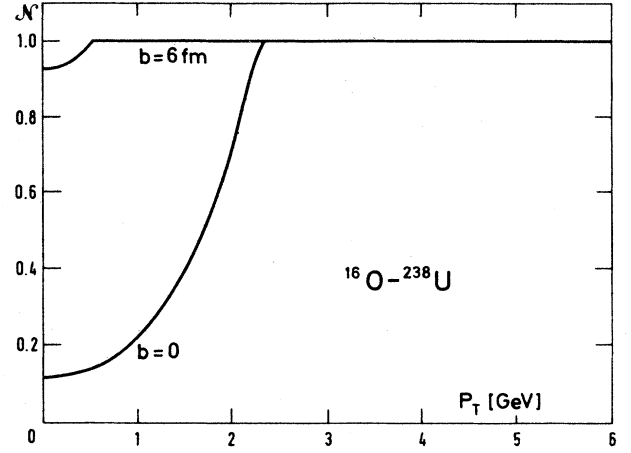


FIG. 13. p_T dependence of J/ψ suppression by a quark-gluon plasma in an oxygen collision, for two values of the impact parameter: $b=0$ (central collision) and $b=6 \text{ fm}$ (peripheral collision). As in Fig. 12, $n_D \tau_\psi = 5.5 \text{ fm}^{-2}$.

cussion in Sec. III. The ratio S_2/S_1 calculated according to Eq. (4.2), separately for pairs with momentum lower than and higher than $1 \text{ GeV}/c$ is 0.42 for $p_T < 1 \text{ GeV}/c$ and 0.81 for $p_T > 1 \text{ GeV}/c$, for an oxygen-uranium collision. These values are somewhat smaller than those extracted from the data.⁵ In the case of a lead-lead collision, displayed in Fig. 15(b), the density is only slightly higher than for an oxygen-uranium collision; but since the variation of \mathcal{N} with the density is so steep in this model, we now obtain considerable suppression, even for rather peripheral collisions.

It should be noted that the screening mechanism tends to give severe J/ψ suppression as soon as the temperature goes over the critical temperature T_D . In other words, the value of \mathcal{N} depends sensitively on the precise value of the parameter $n_D \tau_\psi$. We have computed numerically the variation, near the point $n_D \tau_\psi = 5.5 \text{ fm}^{-2}/c$:

$$\frac{d \ln \mathcal{N}}{d \ln (n_D \tau_\psi)} \simeq 2.3 . \quad (4.6)$$

Things are smoother for the absorption model. There the variation of \mathcal{N} with σ is not too important. Indeed, we get, from Eq. (2.31),

$$\frac{d \ln \mathcal{N}}{d \ln \sigma} = \ln \mathcal{N} \simeq -0.3 . \quad (4.7)$$

That is, our results do not depend crucially on the parameter σ . In fact, there is another parameter on which we have little control in our calculation, which is the initial time t_0 at which absorption starts. If we take a value αt_0 instead of t_0 and keep \mathcal{N} unchanged, we get a new value σ' for the cross section which is easily derived from Eq. (2.31):

$$\frac{\sigma'}{\sigma} = \frac{\ln(t_f/t_0)}{\ln(t_f/\alpha t_0)} . \quad (4.8)$$

For $t_0/t_f \simeq 0.15$ and $\alpha=2$, we get an enhancement of $\sim 60\%$ in the cross section. Thus, the value $\sigma=1.5 \text{ mb}$

which we have used in our calculation should not be considered as a well-determined quantity.

Finally, we have gathered in Table II some predictions of the two models for several nucleus-nucleus collisions at 200 GeV per nucleon. The parameters σ and $n_D \tau_\psi$ have been kept equal to their value chosen for O-U collisions. The main difference between the two models lies in the fact that in the case of inelastic scattering with pions, most of the absorption already takes place in the first transverse-energy bin, and \mathcal{N} remains then roughly constant as one increases the transverse energy. A similar observation was made in a related situation in Ref. 7. On the contrary, the plasma model induces a steep variation of the suppression with transverse energy: except for Pb-Pb collisions, there is no suppression at all in the first transverse-energy bin. In particular, in O-Cu collisions, the initial temperature is not high enough for Debye screening to play any role. Note however, that uncertainties in the formation time of the $c\bar{c}$ pair (our time $t=0$),

or in other times such as τ_ψ , the formation time of the J/ψ , may induce fluctuations which could smoothen this steep variation.

V. CONCLUSIONS

We have presented a detailed study of two possible mechanisms which could account for some suppression of J/ψ production in nucleus-nucleus collisions as compared to proton-proton collisions. These two mechanisms are the absorption of the J/ψ by the dense matter produced in the collision and the Debye screening of the binding potential by a quark-gluon plasma. In both cases we have treated with care the space-time evolution of the system. Even though some rather crude approximations

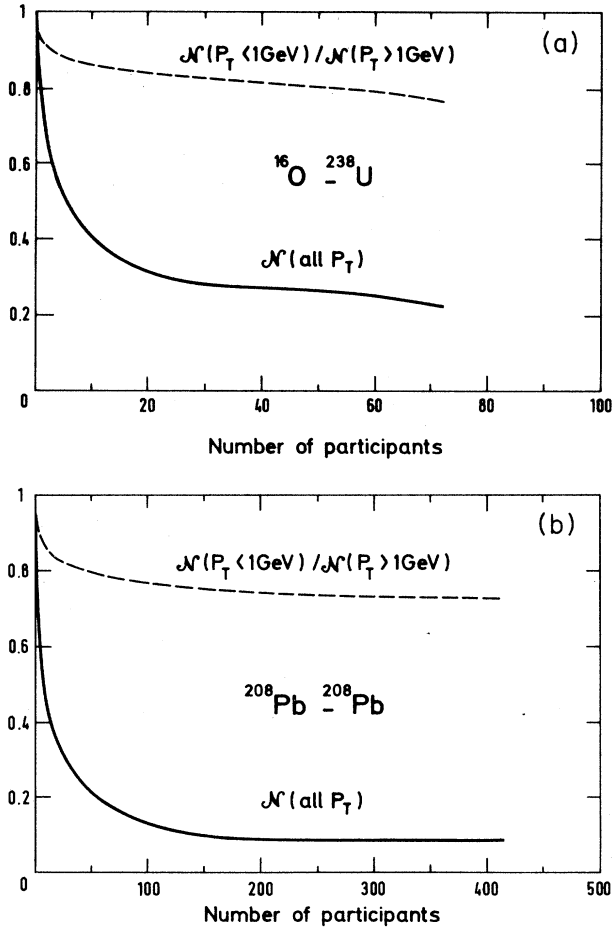


FIG. 14. J/ψ absorption by the pion gas as a function of the number of participants. Solid line: fraction of remaining J/ψ 's, integrated over p_T ; dashed line: comparison between suppression at low p_T and suppression at high p_T . (a) Oxygen-uranium collision; (b) lead-lead collision. As in Figs. 10 and 11, $\sigma=1.5$ mb. The calculations have been done with the following values of the freeze-out time for $b=0$: $t_f/R_0 \approx 1.1$ for low p_T and $t_f/R_0 \approx 0.8$ for large p_T .

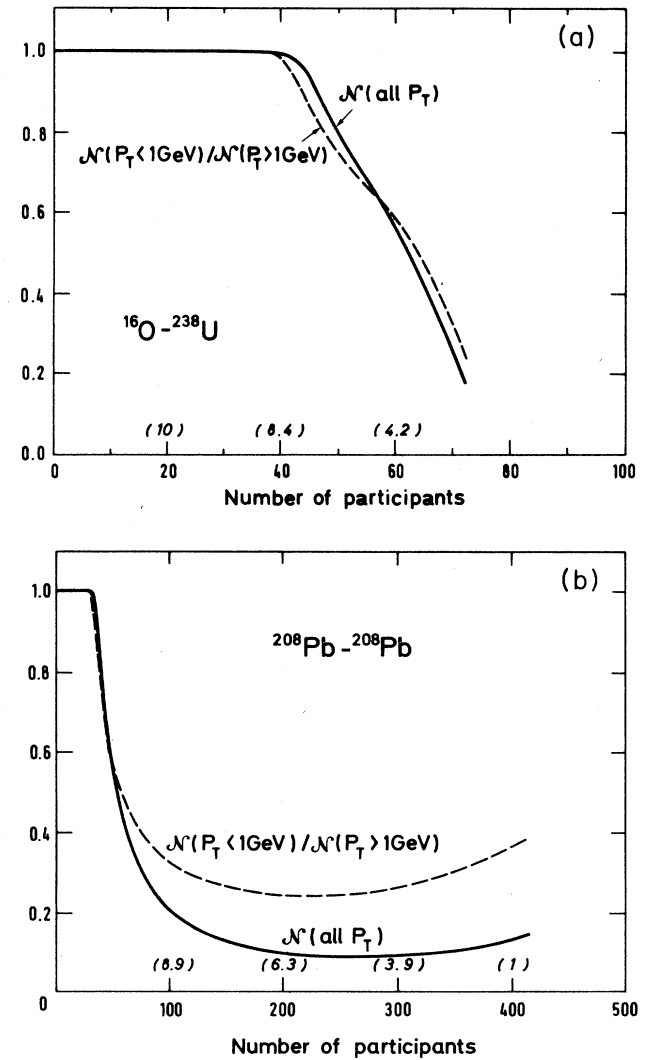


FIG. 15. J/ψ suppression by a quark-gluon plasma, as a function of the number of participants. Solid line: fraction of remaining J/ψ 's, integrated over p_T ; dashed line: ratio of \mathcal{N} integrated over $p_T < 1$ GeV to \mathcal{N} integrated over $p_T > 1$ GeV. (a) Oxygen-uranium collision; (b) lead-lead collision. As in Figs. 12 and 13, $n_D \tau_\psi = 5.5 \text{ fm}^{-2}$ for both curves. Values of the impact parameter b (in fm) are given in parentheses.

have been used, and our comparison with experimental data is still somewhat superficial, a number of conclusions can be drawn from our work and we shall summarize them in this section. Some of them can already be found in Ref. 22.

Let us consider first the absorption mechanism. We have calculated the amount of absorption which could arise because the $c\bar{c}$ system, after it is born, propagates in a dense system of particles (quarks, gluons, hadrons?) also produced in the collision. We have taken into account in our work only that part of the absorption which takes place after the $c\bar{c}$ pair has escaped the baryon-rich region. Absorption by the baryon-rich matter has been considered explicitly in Refs. 6 and 7. We have estimated the effects of the fast dissolution of the matter because of its expansion both in the longitudinal as well as in the transverse directions. Our net result is that the absorption mechanism could account for a substantial suppression of the J/ψ production. One should emphasize, however, that most of the absorption takes place at very short times, that is when the density of hadronic matter is quite

large, so large that it probably does not make sense to think of it as being composed of hadrons only. Note that the parameter which controls the absorption is not the cross section alone, but the product of the cross section by the density of scatterers, and this product may not change drastically as the hadron matter dissolves into a partonic system. In other words, even if some absorption mechanism of the type described in this paper were responsible for the J/ψ suppression, it would still be hard to unambiguously decide the nature of the absorbing medium. Another feature of the absorption mechanism, at least in the way we calculated it, i.e., using a constant cross section, is its very weak dependence on the J/ψ momentum.

The model based on Debye screening does predict a strong dependence on the J/ψ transverse momentum. This is directly related to the short plasma lifetime. When compared with experimental data, it seems to provide an overall better picture. This may look encouraging, but our analysis raises some important questions which should be answered before conclusions could be

TABLE II. (a) Definition of the four transverse-energy bins with equal statistics. N is the total number of participating nucleons and b is the impact parameter, expressed in fm. (b) J/ψ absorption by inelastic scattering on pions, with $\sigma = 1.5$ mb. The numbers in italics (first lines) give the fraction \mathcal{N} of surviving J/ψ 's, averaged over the transverse energy bin. The other numbers are the ratios $\mathcal{N}(i\text{th bin})/\mathcal{N}(\text{first bin})$. For $^{16}\text{O}-^{238}\text{U}$ collisions, these can be compared to the experimental results taken from Ref. 5 (numbers in parentheses). (c) Same as table (b) for J/ψ absorption by a quark-gluon plasma ($n_D\tau_\psi = 5.5 \text{ fm}^{-2}$).

	First bin	Second bin	Third bin	Fourth bin
(a)				
$^{16}\text{O}-^{238}\text{U}$	$N < 38$ $b > 6.1$	$38 < N < 57$ $4.6 < b < 6.1$	$57 < N < 66$ $3.2 < b < 4.6$	$66 < N < 73$ $b < 3.2$
$^{32}\text{S}-^{238}\text{U}$	$N < 57$ $b > 6.4$	$57 < N < 87$ $4.8 < b < 6.4$	$87 < N < 108$ $3.2 < b < 4.8$	$108 < N < 120$ $b < 3.2$
$^{16}\text{O}-^{65}\text{Cu}$	$N < 22$ $b > 4.4$	$22 < N < 34$ $3.2 < b < 4.4$	$34 < N < 44$ $2.1 < b < 3.2$	$44 < N < 51$ $b < 2.1$
$^{208}\text{Pb}-^{208}\text{Pb}$	$N < 144$ $b > 7.7$	$144 < N < 229$ $5.6 < b < 7.7$	$229 < N < 310$ $3.6 < b < 5.6$	$310 < N < 416$ $b < 3.6$
(b)				
$^{16}\text{O}-^{238}\text{U}$	<i>0.30</i> 1 (1)	<i>0.25</i> 0.82 (0.85)	<i>0.23</i> 0.75 (0.80)	<i>0.21</i> 0.69 (0.63)
$^{32}\text{S}-^{238}\text{U}$	<i>0.25</i> 1	<i>0.19</i> 0.77	<i>0.18</i> 0.72	<i>0.17</i> 0.66
$^{16}\text{O}-^{65}\text{Cu}$	<i>0.36</i> 1	<i>0.29</i> 0.81	<i>0.28</i> 0.78	<i>0.27</i> 0.75
$^{208}\text{Pb}-^{208}\text{Pb}$	<i>0.16</i> 1	<i>0.08</i> 0.53	<i>0.08</i> 0.49	<i>0.08</i> 0.49
(c)				
$^{16}\text{O}-^{238}\text{U}$	1 1 (1)	<i>0.94</i> 0.94 (0.85)	<i>0.77</i> 0.77 (0.80)	<i>0.60</i> 0.60 (0.63)
$^{32}\text{S}-^{238}\text{U}$	<i>0.98</i> 1	<i>0.78</i> 0.80	<i>0.62</i> 0.63	<i>0.49</i> 0.50
$^{16}\text{O}-^{65}\text{Cu}$	1 1	1 1	1 1	1 1
$^{208}\text{Pb}-^{208}\text{Pb}$	<i>0.59</i> 1	<i>0.32</i> 0.54	<i>0.27</i> 0.46	<i>0.27</i> 0.46

drawn concerning the formation of a quark-gluon plasma. First of all, it is somewhat unpleasant to find that all the time scales entering the problem are mixed. The J/ψ formation time, the lifetime of the plasma, the formation time of the plasma, the time for the two nuclei to cross each other, all these times end up being of the same order of magnitude, typically 1 fm/c. Certainly one would feel more confident in the overall picture if these various times were clearly separated. Besides, there are times such as the J/ψ formation time, which are really meant to be averages (the formation of a resonance is clearly a quantum-mechanical process and the time that it takes cannot be sharply defined); it is somewhat embarrassing to find a situation where the fluctuations that one could reasonably expect are of the same order of magnitude as the averages themselves. Finally, one could also worry about the validity of the microscopic picture underlying the model. Our results when compared with experiment imply that the J/ψ production is suppressed by a mechanism which takes place at early times, i.e., when the plasma is hot enough. Do the quark and the gluons produced in the collision reach a state of thermal equilibrium quickly enough to allow such a collective effect as Debye screening to set in rapidly? Or is the formation process strongly disturbed by collisions of the charm quarks with the surrounding gluons and light quarks?

The two mechanisms which we have been studying refer, quite generally, to two distinct microscopic pictures. Screening is usually understood as resulting from a collective behavior of the whole system, while absorption is caused by independent collisions of the $c\bar{c}$ system on whatever particles surround it (quarks, gluons, hadrons). If one tries to compare the predictions of the two mechanisms, one finds similarities and differences in their dependence on the total transverse energy of the collision, i.e., the impact parameter, or on the momentum of the J/ψ . We have seen that the absorption depends very smoothly on the impact parameter, while the screening sets in only if the initial density is large enough. However, the fluctuations which could be expected in the various time scales in the problem may partly wash out this threshold effect. The p_T dependence is large in the model based on plasma screening; this p_T dependence originates from combined effects of J/ψ formation time, Lorentz dilation, and plasma finite lifetime. On the other hand, the absorption mechanism was found to depend very little on the J/ψ momentum.

Note added. While this paper was being reviewed for publication, we have estimated the effects of initial-state scatterings on the J/ψ momentum distribution. We find these to be large; they may account for a substantial fraction of the momentum dependence see in the NA38 data.²³

ACKNOWLEDGMENTS

We would like to express our thanks to the members of the NA38 Collaboration, and in particular to C. Gerschel for instructive discussion. We are also grateful to A. Morel for a critical reading of the manuscript. Service de

Physique Théorique is Laboratoire de l'Institut de Recherche du Commissariat à l'Énergie Atomique.

APPENDIX: SIMPLE GEOMETRICAL CONSIDERATIONS

Let us consider the collision of a projectile nucleus of mass number B on a target nucleus of mass number A , with an impact parameter b (see Fig. 16). We call z the coordinate along the collision axis and denote by s the coordinates in the orthogonal directions ("transverse plane"). Let $\rho_A(s, z)$ and $\rho_B(s - \mathbf{b}, z)$ be the density of nucleons in the target and projectile, respectively. Then we define

$$T_A(s) = \int_{-\infty}^{+\infty} \rho_A(s, z) dz \quad (\text{A1})$$

and similarly for the nucleus B . For a nucleus with a uniform density inside a sphere of radius $R_A = r_0 A^{1/3}$ ($r_0 = 1.2$ fm), one has

$$T_A(s) = \frac{2}{3\pi r_0^3} (R_A^2 - s^2)^{1/2}. \quad (\text{A2})$$

In order to estimate the average number of participating nucleons in a nucleus-nucleus collision at impact parameter b , we assume that all the nucleons of the projectile (target) that cross the target (projectile) nucleus interact. That is, all the nucleons which are in the surface S_{eff} where the two nuclei overlap in the transverse plane (crosshatched region in Fig. 16) undergo at least one inelastic collision. Thus, the density of participating nucleons per unit area d^2s is simply $T_A(s) + T_B(s - \mathbf{b})$ in S_{eff} , and 0 outside. The total number of participants

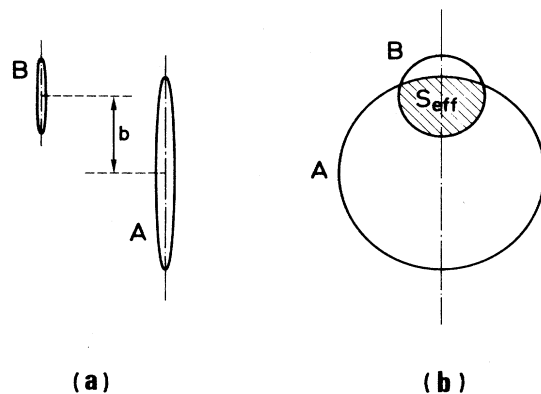


FIG. 16. Picture of a peripheral oxygen-uranium collision ($R_B \approx 3$ fm, $R_A \approx 7.4$ fm) with impact parameter $b = 6$ fm. (a) View of the collision in the plane of incidence, in the nucleon-nucleon center-of-mass frame: the two nuclei are Lorentz contracted by a factor $\gamma = 10$. (b) View in the transverse plane: the region where the nuclei overlap, which is the region of interaction, has been crosshatched; its area is the quantity S_{eff} .

$N(b)$ obtained after integration over s , is displayed in Fig. 17 as a function of the impact parameter. In the case of oxygen-uranium collisions [Fig. 17(a)] one sees that when $b < R_A - R_B \simeq 4.4$ fm, all the nucleons in the oxygen nucleus participate. If one assumes that the total transverse energy produced in the collision is directly proportional to the number of participants, with an average energy per participant E_0 , one obtains a simple geometrical description of the transverse-energy distribution:

$$\frac{d\sigma}{dE_T} = \frac{2\pi b db}{E_0 dN(b)}. \quad (\text{A3})$$

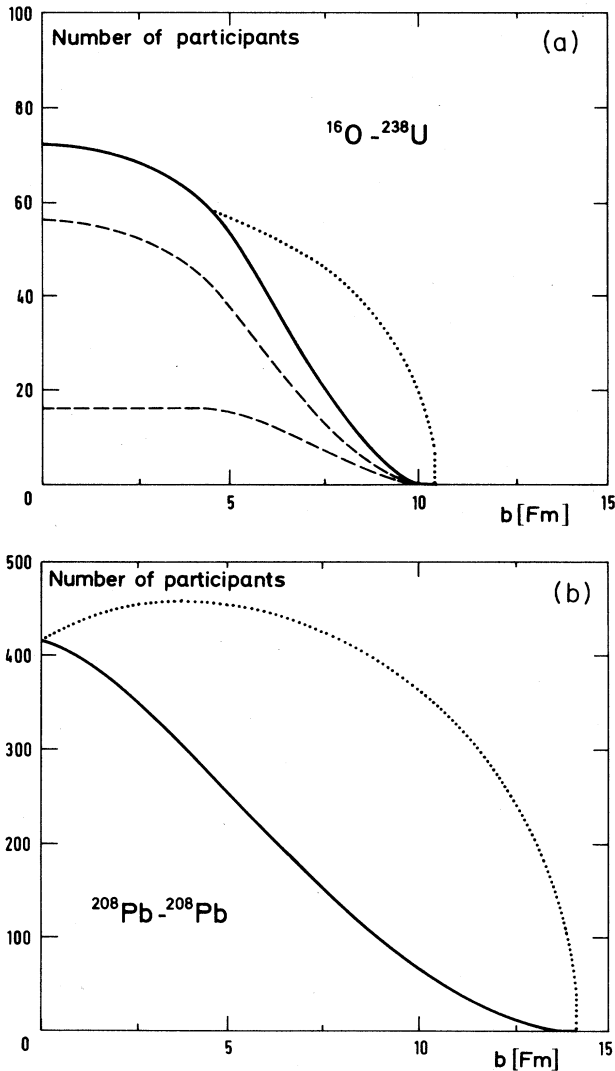


FIG. 17. Number of participants as a function of the impact parameter: (a) oxygen-uranium collision: the number of participating nucleons from oxygen and uranium are displayed separately (dashed curves); the total number of participants is the solid curve; the dotted curve is the product of the number of participants by the quantity $\pi R_B^2/S_{\text{eff}}$. (b) Lead-lead collision: the solid curve is the total number of participants, which is multiplied by $\pi R_B^2/S_{\text{eff}}$ in the dotted curve.

This distribution reproduces the bulk features of the measured distributions.²⁰

It is also commonly accepted that the multiplicity of particles produced in the central rapidity region is proportional to the number of participants. Let $(dN/dy)_0$ be the multiplicity density per participant. From Ref. 21 one gets $(dN/dy)_0 \simeq 2.3$. We then estimate the density of particles per unit area, at time t_0 , with the formula

$$n(s, t_0) t_0 = \left[\frac{dN}{dy} \right]_0 [T_A(s) + T_B(s-b)]. \quad (\text{A4})$$

When T_A and T_B are given by Eq. (A2) and in the case of a central collision of identical nuclei, Eq. (A4) gives the distribution (2.23) with $a = \frac{1}{2}$. The mean value n_0 of $n(s, t_0)$ in the surface of interaction is obviously given by $n_0 t_0 = (1/S_{\text{eff}}) dN/dy$. For a central collision with $B \ll A$, the total number of participants is $N(b=0) = B + \frac{3}{2} B^{2/3} A^{1/3}$. This yields

$$\frac{1}{S_{\text{eff}}} \frac{dN}{dy} = \frac{1}{\pi r_0^2} \left[\frac{dN}{dy} \right]_0 (B^{1/3} + \frac{3}{2} A^{1/3}). \quad (\text{A5})$$

In Fig. 17 we also show the product of the number of participants by the quantity $\pi R_B^2/S_{\text{eff}}$. The quantity thus obtained is directly proportional to $(1/S_{\text{eff}}) dN/dy$. In the case of an oxygen-uranium collision [Fig. 17(a)], it is a monotonously decreasing function of b , which is equal to the number of participants when $b < R_A - R_B$, since then $S_{\text{eff}} = \pi R_B^2$; when $b > R_A - R_B$, it is bigger than the number of participants since $S_{\text{eff}} < \pi R_B^2$. On the contrary, we see that for a collision of two identical nuclei such as lead [Fig. 17(b)], the maximum of $(1/S_{\text{eff}}) dN/dy$ is obtained for a nonzero impact-parameter ($b \simeq 3.6$ fm for lead). This maximum value, which is easily calculated from Fig. 17, is found to be 5.7 fm^{-2} for an oxygen-uranium collision and 6.8 fm^{-2} for a lead-lead collision.

With regards to the production of $c\bar{c}$ pairs, we assume that it is proportional to the number of individual nucleon-nucleon collisions. More precisely, we assume that the probability to create a $c\bar{c}$ pair per unit area d^2s is proportional to the product $T_A(s)T_B(s-b)$. Therefore, the distribution function for $c\bar{c}$ pairs at time $t=0$ is taken of the form

$$f_0(s) \propto T_A(s)T_B(s-b). \quad (\text{A6})$$

For a central collision of identical nuclei, and with T_A and T_B given by (A2), Eq. (A6) reduces to Eq. (2.22) with $b=1$. For a small projectile colliding with a large target at zero impact parameter, T_A is almost constant over the region of interaction, and (A6) is equivalent to (2.22) with $b = \frac{1}{2}$. The total number of nucleon-nucleon collisions at impact parameter b is proportional to $T_{AB}(b)$ where

$$T_{AB}(b) = \int d^2s T_A(s)T_B(s-b). \quad (\text{A7})$$

- ¹T. Matsui and H. Satz, Phys. Lett. B **178**, 416 (1986).
²F. Karsch and R. Petronzio, Phys. Lett. B **193**, 105 (1987).
³J. P. Blaizot and J. Y. Ollitrault, Phys. Lett. B **199**, 499 (1987).
⁴M. C. Chu and T. Matsui, Phys. Rev. D **37**, 1851 (1988); P. V. Ruuskanen and H. Satz, Z. Phys. C **37**, 623 (1988).
⁵NA38 Collaboration, M. C. Abreu *et al.*, in *Quark Matter '87*, proceedings of the Sixth International Conference on Ultrarelativistic Heavy Ion Collisions, Nordkirchen, Federal Republic of Germany, edited by H. Satz, H. J. Specht, and R. Stock [Z. Phys. C **38**, 117 (1988)].
⁶C. Gerschel and J. Hüfner, Phys. Lett. B **207**, 253 (1988).
⁷A. Capella *et al.*, Phys. Lett. B **206**, 354 (1988).
⁸J. Ftacnik, P. Lichard, and J. Pisut, Phys. Lett. B **207**, 194 (1988).
⁹S. Gavin, M. Gyulassy, and A. Jackson, Phys. Lett. B **207**, 257 (1988).
¹⁰R. Vogt, M. Prakash, P. Koch, and T. H. Hansson, Phys. Lett. B **207**, 263 (1988).
¹¹B. Svetitsky, Phys. Rev. D **37**, 1581 (1988).
¹²R. V. Gavai and S. Gupta, Report No. TIFR/TH/88-18 (unpublished).
¹³NA3 Collaboration, J. Badier *et al.*, Z. Phys. C **20**, 101 (1983).
¹⁴S. J. Brodsky and A. H. Mueller, Phys. Lett. B **206**, 685 (1988).
¹⁵J. Ranft, Phys. Rev. D **37**, 1842 (1988).
¹⁶J. D. Bjorken, Phys. Rev. D **27**, 140 (1983).
¹⁷G. Baym, B. L. Friman, J. P. Blaizot, M. Soyeur, and W. Czyz, Nucl. Phys. A **407**, 541 (1983).
¹⁸J. P. Blaizot and J. Y. Ollitrault, Nucl. Phys. A **458**, 745 (1986); J. Y. Ollitrault, in *Hadrons, Quarks and Gluons*, proceedings of the XXIInd Rencontre de Moriond, Les Arcs, France, 1987, edited by J. Tran Thanh Van (Editions Frontières, Gif-sur-Yvette, 1987), pp. 495–501.
¹⁹F. Karsch, M. T. Mehr, and H. Satz, Z. Phys. C **37**, 617 (1988).
²⁰WA80 Collaboration, R. Albrecht *et al.*, Phys. Lett. B **199**, 297 (1987).
²¹NA35 Collaboration, H. Ströbele *et al.*, Z. Phys. C **38**, 89 (1988).
²²J. P. Blaizot, in *Quark-Gluon Plasma*, proceedings of the International Conference on Physics and Astrophysics, Bombay, India, 1988, edited by B. Sinha and S. Raha (World Scientific, Singapore, in press).
²³J. P. Blaizot and J. Y. Ollitrault, BNL Report No. 41759, 1988 (unpublished).